An experimental investigation into the behaviour of bidisperse granular avalanches

Performed at the University of Cambridge

Elze Porte, s1012436
August 2014
University of Twente

Preface

I have to agree with Yair Srebro and Dov Levine who said that "the tendency towards segregation in granular mixtures (...) is interesting for the physicist and disturbing for the engineer". Nevertheless, still considering myself an engineer, I developed a great interest in the behaviour of segregating flows and enjoyed gaining understanding of this complicated phenomenon and its consequences.

I would like to thank the Fluid Mechanics research group at the University of Cambridge for letting me use their facilities. In particular, I would like to thank Dr. Nathalie Vriend for being a helpful and inspiring supervisor. I appreciate the support she has given me throughout the internship and the opportunity she gave me to assist with field work in Austria.

Nomenclature

Symbol	Description	Unit
θ	Angle of inclination	-
θ_1	Minimum angle for flow	-
θ_2	Maximum angle with a flow deposit	-
μ_b	Basal friction	-
d	Particle diameter	mm
d_c	Critical diameter at which basal friction is maximum	mm
h_{stop}	Deposit thickness	mm
L	Characteristic dimensionless thickness	-
Q	Mass flux	kg/s
R	Kinetic energy associated with random particle movements	J
t	Time	s
U	Flow velocity	m/s

Contents

Chapter 1

Introduction

Granular flows cover a variety of appearances in a variety of circumstances. Snow avalanches and rock slides are among the natural granular flows and granular flows appear in industry when particles are transported. Even though the size and shape of the material differ among the different types of flows, some phenomena appear in any of these flows. Among these phenomena is the formation of levees. When a flow comprises at least two sizes of particles, size segregation is clearly visible since the large particles accumulate on the side and front of the flow forming the levees.

In previous attempts to study the formation of levees, at the University of Cambridge, the reproducibility proved to be critical in setting up experiments. The angle of repose and the alteration of the reservoir size were used in a first attempt to find a setup with reproducible flows, described in *The angle of repose and the alteration of volume*. Since this study was insufficient to set up reproducible experiments, a slightly different approach is used in this investigation. Instead of studying the mutual friction between particles (angle of repose) the frictional behaviour on a specific roughness is studied. The main purpose of this investigation is to gain insight in the specific behaviour of the particles available in the laboratory in Cambridge.

The basal friction is experimentally determined, according to the method of Pouliquen [1], in order to be able to predict instabilities. Additional experiments with bidisperse mixtures of the available particles, mimicking a study of Goujon et al. [2], are used to support the prediction of instabilities and investigate the significance of increased flow mobility on the reproducibility of experiments. The results of the experiments are expected to fit with the conclusions of earlier research [1, 2].

This report starts with a literature study into several phenomena in monodisperse and bidisperse flows. Among the topics are the formation of levees, size segregation and effects of basal friction. The chapter *Hypotheses* shortly reflects on how the theory is expected to relate to in the results. The method of the experimental research, like setup, particles and settings as well as the method of data analysis are described in the *Methods* section. The results are presented in the chapter *Results*. Further, the *Discussion* reflects on the procedures and results. Results of the individual experimental are linked in the *Conclusion* and the relevance of the results is discussed. The report finishes with a personal reflection on the internship.

Chapter 2

Theory

The theory in this chapter supports and initiates the performed experiments. First, the monodisperse flows and subsequently the bidisperse flows are discussed . In both cases the formation of levees is included even though no experiments were performed to study this phenomenon. However, the study to the formation of levees initiated this research, so the theory is included for future purposes. Another intention of the given theory is offering a next student a head start on the studied topics.

2.1 Monodisperse flows

The focus of the theory of the monodisperse flows is the basal friction. The deposit thickness relates to the magnitude of the friction between the particles and the base. In addition, a critical particle diameter exist for which the basal friction is maximum. The monodisperse section finishes with some theory on the formation of levees.

2.1.1 Friction between a rough base and avalanching particles

The basal friction is an important factor to take into account when studying the deposition behaviour of a flow. Pouliquen [1] shows that this friction between the rough surface and the particles flowing down determines the deposit thickness, h_{stop}, at a certain angle. Different combinations of roughness of the base and particle size result in different h_{stop} behaviour, as shown in figure 2.1(a).

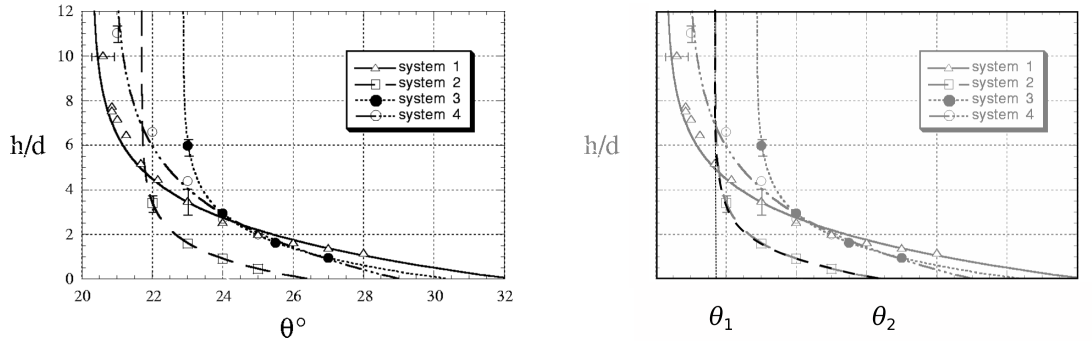

(a) Results from Pouliquen [1]

(b) Results showing θ_1 and θ_2, adapted from [1]

Figure 2.1: h_{stop} as a function of θ for four different systems

Each system represents a different combination of the size of the flowing particles and the size of the particles glued to a surface, forming a rough base. System 2, 3 and 4 use the same rough surface and only differ in the size of the flowing particles. System 1 uses the same particles as system 4, but on a surface with another roughness.

All of the h_{stop} curves show a minimum angle, θ_1, and maximum angle, θ_2, for which stationary flow is possible, as drawn in figure 2.1(b). In case $\theta < \theta_1$ no stationary flow is possible and

mathematically h_{stop} tends to infinity. No particle stays on the plane when $\theta > \theta_2$, since h_{stop} is always zero beyond that point. A good fit for any of these h_{stop} curves is given by [1] as:

$$\tan\theta = \tan\theta_1 + (\tan\theta_2 - \tan\theta_1)\exp\left(-\frac{h_{stop}}{Ld}\right), \tag{2.1}$$

where d is the particle diameter and L is a characteristic dimensionless thickness over which θ_{stop}(h) varies. L is not explicitly calculated, but probably determined by

$$L = \frac{h_{stop}(\theta_1)}{\theta_2 - \theta_1}, \tag{2.2}$$

where h_{stop} is already dimensionless.

Goujon et al. [3] use three criteria to determine the critical particle diameter d_c for which the basal friction reaches a maximum:

- the thickness of the deposit (h_{stop}) is maximum;
- the length of the deposit is minimum;
- the velocity of the non-uniform steady-state flow is minimum.

Applying these criteria to their results shosw d_c is independent of the inclination of the chute and is about $^1/_2$ the size of the roughness of the base.

2.1.2 Formation of levees

The flowing and stopping phase of a flow is separated by a mathematical saddle point equilibrium [4]. The relation between the kinetic energy associated with random particle movements (R) and the flow velocity (U) has a saddle point equilibrium. The distance of the saddle point from the centre of the flow as a fraction of the width of the flow is dependent on the mean mass flux, $\bar{Q}$. For large $\bar{Q}$ the distance is about half of the flow width. Hence, the mean mass flux determines the width of the levees relative to the width of the flow.

The height of levees is linked to the flow front height. Whilst the particles flow down, static borders form along the side of the flow [5, 6]. When the supply stops the height of the static borders remains unchanged and only the height in the channel decreases. Since the height of the static borders is initially close to the height of the flow front, the height of the levees of the deposit is linked to the initial front height.

In addition, Deboeuf et al. [6] state that the levee thickness also dependents on the flow duration t. For increasing t, the levee thickness decreases until the levee vanishes and the deposit of the flow is of equal height. Another effect of an increased flow duration is the widening of the flow. Figure 2.2 on the following page shows that the flow widens and decreases in height until the height of the flow is equal to h_{stop}. At this point the channel height does not decrease when the supply stops, so the static borders do not differ in height with the channel.

Takagi et al. [7] are in agreement with the statement of Deboeuf et al. [6] that both the flow thickness and the flow width depend on the flow duration and reach a constant value with time. On the other hand, Takagi et al. [7] show in their experimental study that the thickness of the flow is never equal over the total flow width (figure 2.3). However, the studies differ not only in the used granular material but also in the duration of the experiments. Where Deboeuf et al. [6] perform experiments with glass beads for up to 600 seconds, Takagi et al. [7] run experiments with sand for over 2 hours.

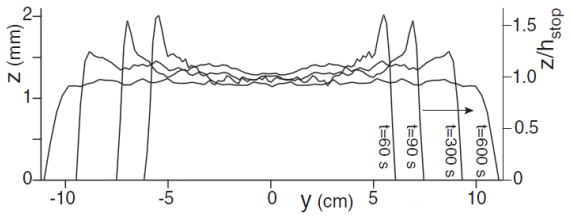

Figure 2.2: Thickness profiles of the flow after different flow durations, reproduced from [6]

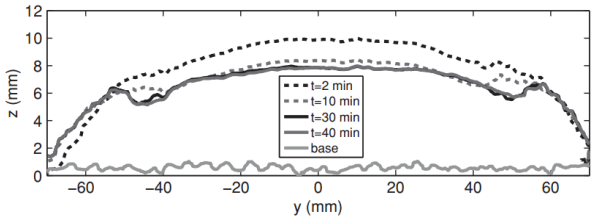

Figure 2.3: Thickness profiles of the flow after different flow durations, reproduced from [7]

2.2 Bidisperse flows

Bidisperse avalanches behave differently from monodisperse avalanches. The theory of several phenomena typically occurring in bidisperse flows are featured in this section. In any bidisperse mixture the particles segregate on based on size. Further, instabilities (or fingering) occur more often in mixtures than in homogeneous samples. The length of the deposits is also influenced by the configuration of a sample. Bidisperse samples have an increased mobility in comparison with either monodisperse sample of the mixture. Finally, some theory of the formation of levees in bidisperse flows is added. Again, this theory is not used in any experiments performed in this research, but is added for future reference.

2.2.1 Size segregation in avalanching flows

Savage and Lun [8] proposed two main mechanisms responsible for particle size segregation in inclined chute flows. The first mechanism is kinetic sieving, sometimes refered to as the 'Brazil nut effect'. However, to physically justify the correctness of this mechanism a second theory was needed. Therefore Savage and Lun [8] established the squeeze expulsion theory. Even so, they mention that "the correctness of details of the physical explanation of this second mechanism is not essential."

The theory of kinetic sieving is based on the probability of particles filling void spaces. The process is visualised in figure 2.4. While the particles flow down (2.4(a)), small particles are more likely to fit into one of the open spaces (2.4(b)) in underlying layers than larger particles. As a result, the flow segregates while it flows further down the slope (2.4(c)).

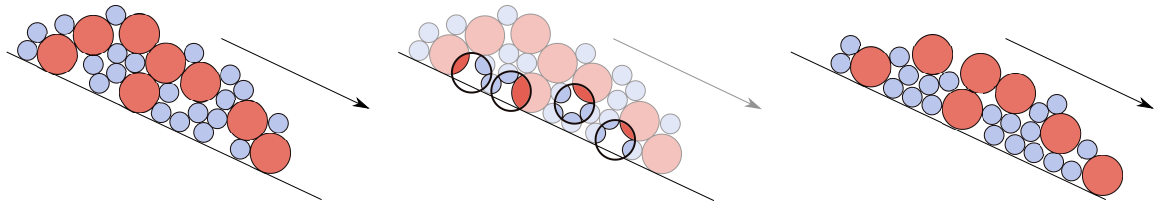

(a) Avalanching flow (b) Vacancies in flow (c) Segregating flow

Figure 2.4: Principle of kinetic sieving

The kinetic sieving theory by itself is insufficient, for it suggests a net mass flux in the z-direction

of the flow. The squeeze expulsion mechanism complements the kinetic sieving theory, for it ensures a zero net mass flux. Figure 2.5 shows this mechanism of squeeze expulsion. Fluctuating contact forces result in force imbalances (2.5(a)), which leads to the distribution of particles to adjacent layers (2.5(b)) [8]. This mechanism applies to the big particles as well as the small particles in a mixture and is not gravity driven.

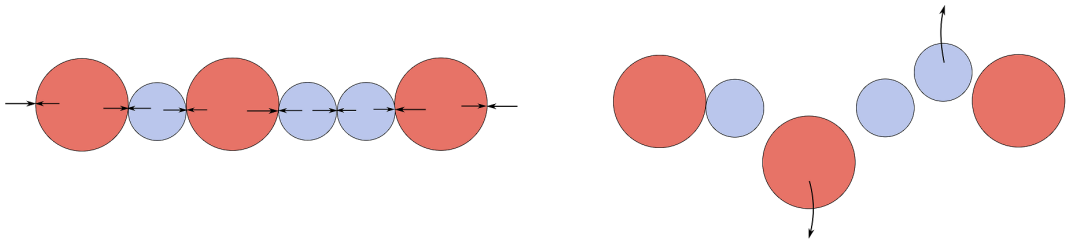

(a) Particle contact forces

(b) Particles squeezed to subsequent layer i.e. both small and large particles could move up- as well as downwards

Figure 2.5: Principle of squeeze expulsion

Ever since the theory of kinetic sieving and squeeze expulsion has been established the mechanism of segregation has been studied elaborately [9–15]. More detailed theories for multi-component flows [9] and time-dependent solutions [10] are established. More extensive studies include recirculation, remixing and depositing of particles [11–13].

2.2.2 Formation of levees

In segregating flows levees channel the flow such that the interior flow level of small or fine particles is lower than the level of the head and sides containing large or coarse particles [16,18]. The internal structure is believed to remain unchanged during the flow. Only when the the flow wanes, the shape of the levees changes to narrow and angular walls, as shown in figure 2.6.

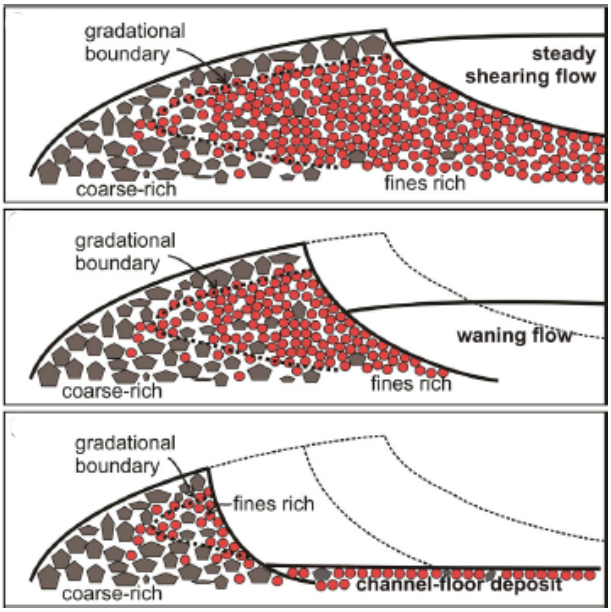

Figure 2.6: Schematic transverse cross sections illustrating structure change in waning flow by [16]

In flows with a mixture of coarse and fine grains the levees seem to consist of merely coarse particles, due to its outer appearance. Nevertheless, cross sectional studies by Kokelaar et

al. [16] show that fine grains are present in the interior of the levees. In addition, Bartelt et al. [17] state that in snow avalanches the particle size distribution of the levees is the same as in the front of the channelized flow.

2.2.3 Instabilities

Size segregation can cause instabilities in granular flows. When large particles accumulate at the front of the flow it is possible the interior, comprising small particles, breaks through this barrier and forms a finger. When the large particles have a larger coefficient of friction they are pushed down slope by the small particle with a small friction coefficient and the barrier becomes unstable because of the pressure from behind [2,19]. The resistance of the barrier to move along or to break depends on the ratio of small and large particles [2].

2.2.4 Increased mobility

Bidisperse flows can have an increased mobility with respect to their monodisperse equivalents [2,20,21]. Small particles at the base of the flow increase the rolling-type interactions and therefore reduce the global friction of the flow [20]. A reduction of the global friction results in an increased mobility and thus runout length. Also, in bidisperse flows with coarse and fine particles the increase of rolling motion due to the presence of fine particles can increase the mobility of a flow [21].

Goujon et al. [2] describe the increased mobility by the interaction between the layers of small and large beads. The large particles on top of the flow scrape on the layer of small particles underneath, resulting in large beads slowing down and small beads speeding up. As a consequence, the mean velocity is larger than in the monodisperse case, causing a decrease of the deposit thickness and increase of the runout length [2].

Chapter 3

Hypotheses

On the basis of the theory several hypotheses about the behaviour of the flows in this study are established. The first four hypotheses relate to monodisperse flows and the final two are applicable to bidisperse flows.

The hypotheses comprises the following statements :

- Each sample shows decreasing deposit thickness with increasing inclination, following to the trend described in [1]
- A critical particle diameter d_c for which the basal friction is maximum exists;
- The critical particle diameter is around half the roughness of the base;
- Particles with diameters larger than d_c have decreasing basal friction with increasing diameter;
- Deposits of bidisperse flows show increased mobility with respect to their monodisperse samples;
- If the basal friciton of the large beads is larger than the basal friction of the small beads one or more fingers appear in the flow.

Chapter 4

Methods

This chapter starts with describing the specifications of the general experimental setup. Subsequently, specific settings for different experiments are presented. Finally, the method for analysing the laser scanner data is explained and justified. A detailed guide of all the steps preparing the setup and performing the experiment is added in Appendix B.

4.1 Experimental setup

Several experiments were performed using the same equipment. A general description of the equipment is given and all the settings for a specific experiment are described in the matching sections.

4.1.1 Equipment

An overview of the chute is given in figure 4.1. All experiments are performed on a 2.6 meter long and 1.0 meter wide chute. The base of the chute is covered with sand paper with a roughness of 425 μm. The inclination θ of the chute can be set with a precision of 0.1°.

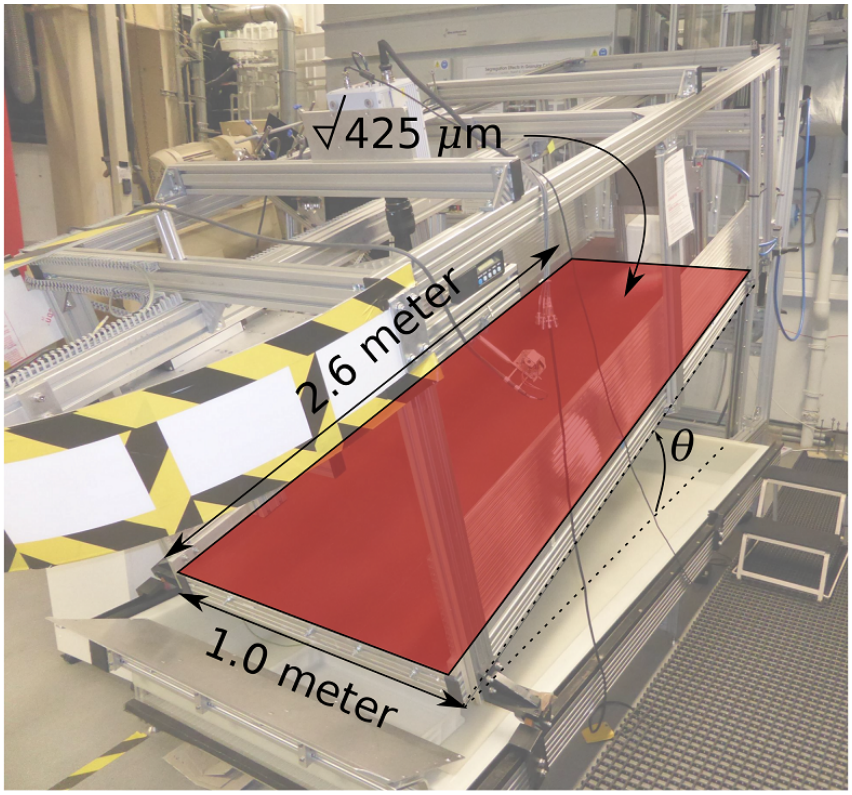

Figure 4.1: Chute overview

A compartment on top of the chute holds the ballotini before release (figure 4.2). The dimensions are 30 x 30 x 25 cm, but can be altered by inserting polystyrene blocks, figure 4.2(a). To avoid ballotini sticking to the polystyrene walls, they are wrapped in paper. On the side facing

down slope, a gate closes the reservoir. Lifting this gate instantly releases the ballotini. To release the ballotini more gradually, an adjustable barrier can be installed. The barrier leaves a slit up to 4 cm free for flow. Inserting the second gate reduces the compartment length with about 8 mm. The barrier itself is 6 mm thick and the gap between the two gates is about 2 mm.

(a) Compartment external overview

(b) Compartment size decreased with polystyrene inserts

Figure 4.2: Compartment overview

A laser scanner is used to gather data about the profile of the deposit. The used scanner is the Micro-Epsilon LLT2800-100. The laser scanner is mounted on a traverse, so it can be moved along the chute. The home position of the traverse is about 23 cm from the compartment gate. Additional information about the working principle and specifications of the laser scanner are added in Appendix B.

4.1.2 Particles

The particles which are used in the several experiments are shown in figure 4.3. Two of the particle samples are colored red (Figures 4.3(a) and 4.3(e)) while the other three samples are plain glass and appear to be white (Figures 4.3(b), 4.3(c) and 4.3(d)). To see a clear distinction between the small and large particles in an experiment a mixture always contains a white and a red sample.

All particles are shaped spherically, but in each sample some deviations are visible. Especially the 0.15 - 0.25 mm sample (figure 4.3(b)) contains a lot of oddly shaped particles. The 0.30 - 0.40 mm (figure 4.3(c)) and the 0.40 - 0.60 mm (figure 4.3(d)) have some particles deviating from a spherical shape, but overall the particles are fairly round and in no case angular. The red samples (0.09 - 0.15 mm and 1.00 - 1.3 mm in Figures 4.3(a) and 4.3(e)) seem to have almost perfectly spherical particles.

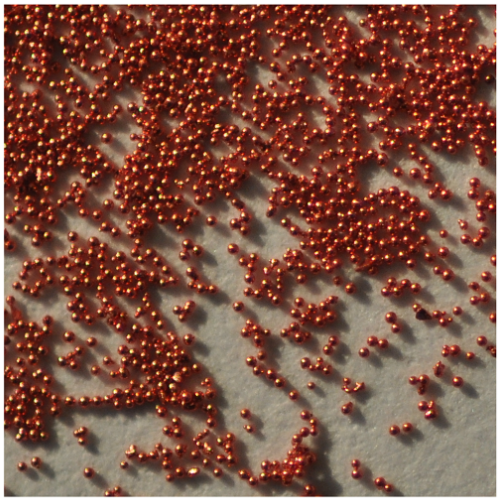

(a) 0.09 - 0.15 mm

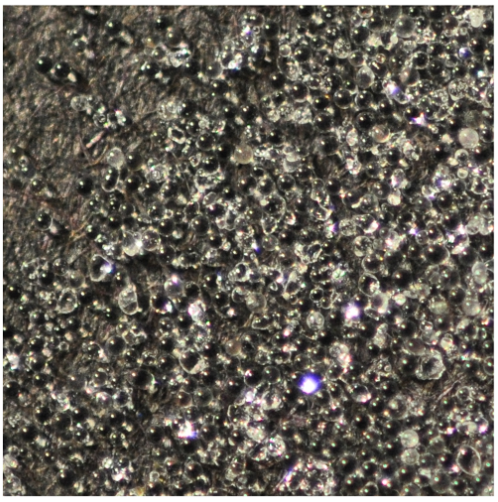

(b) 0.15 - 0.25 mm

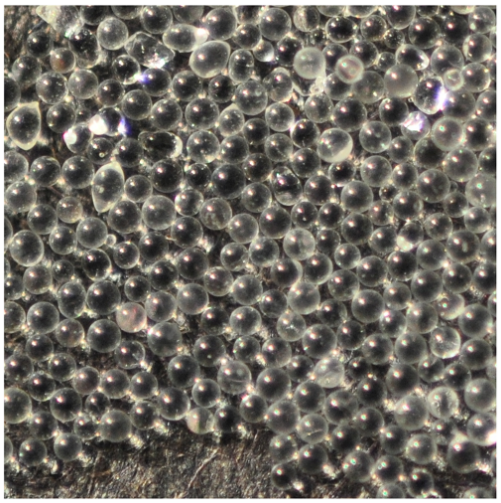

(c) 0.30 - 0.40 mm

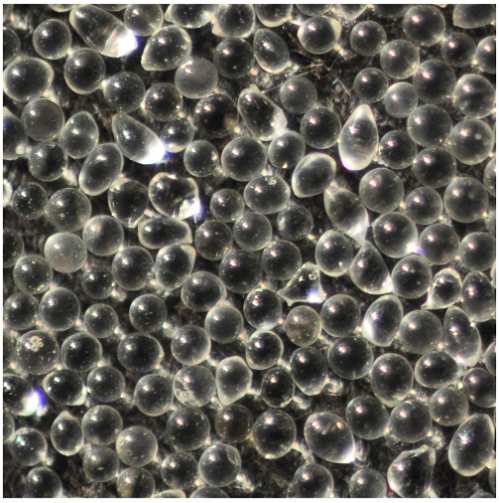

(d) 0.40 - 0.60 mm

(e) 1.00 - 1.3 mm

Figure 4.3: Particles

4.1.3 Basal friction

The goal of the investigation of the basal friction is to select an angle of inclination for further experimentation which is larger than θ_1 and smaller than θ_2 for all sizes of ballotini.

The angle of repose is used as the basis for the measurements. The angle of repose is the angle at which the material is at the verge of sliding in heaps of granular material. The angle at which the material starts flowing on the chute may differ from its angle of repose, but the angles are expected to be very similar. The angle of repose for the different sizes of ballotini is determined in a previous study by the author *(The angle of repose and the alteration of volume)* and the results are repeated in figure 4.4. Only the angle of repose for the 0.09 - 0.15 mm ballotini is unknown. The results show that the angle of friction is not a function of the particle size, but rather depends on the angulartiy of the particles.

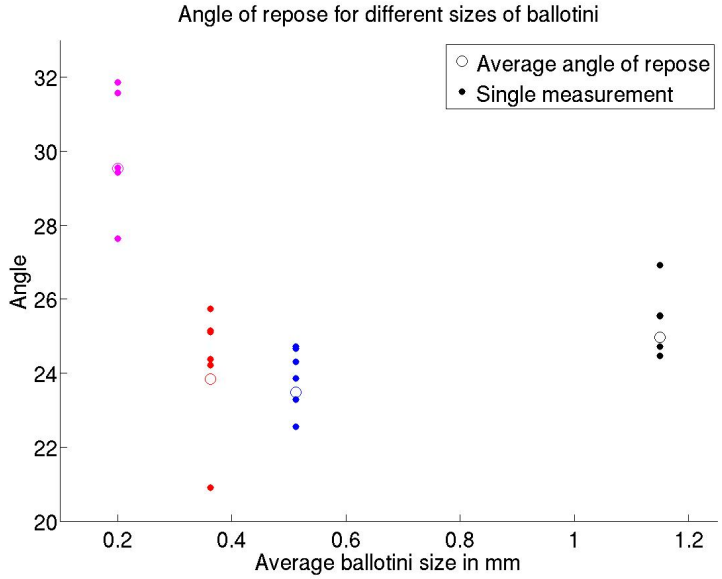

Figure 4.4: Results from previous experiments to investigate the angle of repose, reproduced from *(The angle of repose and the alteration of volume)*

The ballotini with the lowest and the highest angle of repose determine the minimum and maximum angle θ for which $\theta_1 < \theta < \theta_2$ holds for any sample. The angle of repose of the 0.15 - 0.25 mm and the 0.40 - 0.60 mm ballotini are furthest apart. So, if an angle θ exists for these samples at which $\theta_1 < \theta < \theta_2$ holds, it will hold for any of the other samples as well. Additional experiments with the other ballotini sizes have to confirm this statement. Details of the settings for each individual experiment are listed in Appendix B.

Measurements for the 0.15 - 0.25 mm and 0.40 - 0.60 mm ballotini are carried out with an interval of 2° until no deposit is left on the chute. Subsequent measurements with the other sizes are taken for at least three angles per size sample. All experiments are performed three times.

4.1.4 Increased mobility and instabilities in bidisperse flows

Several experiments are carried out to study the frictional behaviour of the monodisperse as well as the bidisperse samples. The maximum runout length and the maximum deposit width are measured and pictures are taken to compare the different samples on their deposit shapes. Each sample is used three times to test the sample on reproducibility and to make the individual

measurements more reliable.

On the basis of the results of the experiments for basal friction, the inclination of the chute is set to 25°. In every case the dimensions of the compartment are reduced to $^1/_2$ its length and $^1/_3$ its width. The reservoir is filled with 1.00 kg ballotini and all mixtures contains 50% large and 50% small particles. The influence of the slit height on the flow is not tested in case of bidisperse samples, so the largest slit height possible (4.0 cm) is chosen to limit possible influences.

The maximum length and width of the deposit are measured with a tapeline. Each individual experiment is photographed with small checked squares on the sides. These squares are useful in processing the pictures, since they determine a straight line down the chute. Some small deviations in the optical length and width of the deposit may have occurred during post processing the images. The pictures in this report can therefore only be used for explanatory purposes and should be supported with the measurement data.

4.1.5 Levee formation

The experiments to investigate the formation of levees were not performed due to the non-reproducible results in the current setup. Appendix C contains a research proposal for a study in the formation of levees. This proposal may be useful as a starting point or a source of inspiration if research on levees is continued. The proposal is only a first draft, so it should by no means be used as a full research proposal.

4.2 Data analysis

This section elaborates on the analysis of the data gathered from measurements with the laser scanner. Several steps of the analysis process are explained and some supporting figures are presented.

4.2.1 Analysing the deposit thickness

The deposit thickness is calculated by subtracting the data from a measurement of a deposit with the data from a measurement of a clear base (without any deposit). It is not possible to measure the deposit thickness directly, because the laser scanner measures the distance from itself to an object. Therefore a measurement of a clear base serves as reference.

The first step in this process is removing all the 'Not a Number' data from the data files. An equal amount of data points in the reference data and the deposit data is maintained by removing the same data points from each file, e.g. if in the reference data contains 'Not a Number' at data point 276, in the deposit data file the data point at the same location is removed.

Each reference data point is subtracted from corresponding data point in the deposit data. After this manipulation the plotted result shows a more or less straight line, representing the thickness of the deposit. The average of the thickness over the length of the measurement area displays h_{stop}. Another method would be to subtract the averages of both data files. This method should result in the same h_{stop}, since only the order of manipulations is changed. Both methods are equally valid and demand about the same process. The firstly described method is chosen, but the second method should have the same result.

4.2.2 Analysing the measurement error

The standard deviation of the measurement determines the error of the results. Figure 4.5(a) shows the validation of the use of the standard deviation to analyse the data files. The dashed line shows a perfect normal distribution, so if the data points coincide with this line the distribution of the data is normal. In this case the data of the measurement have a very good fit with a normal distribution. The use of the standard deviation is therefore justified.

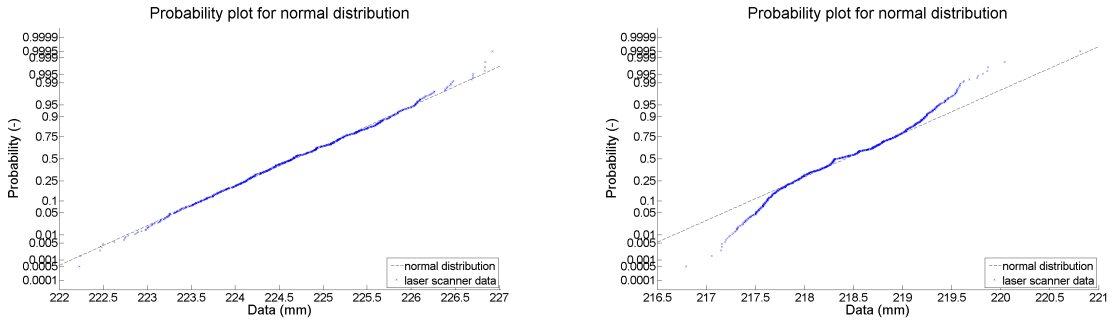

(a) Validation of using a standard deviation

(b) Deviating data from a normal distribution

Figure 4.5: Probability plots of a normal distribution

Not all data files show a fit as close to the normal distribution as in figure 4.5(a). The probability plot in figure 4.5(b) shows that the data seems symmetrically distributed, but does not fit a perfect normal distribution. At the lower end and upper end of the data spectrum show respectively smaller and higher probabilities compared to a normal distribution, which means the variance is smaller. This discrepancy means that the approximated error (the standard deviation) is higher than the actual error, making it a conservative rather than incorrect assessment of error.

To calculate the error over the average h_{stop}, the average deviation of the individual measurements is taken. Only three different deposits are measured, which is a rather small amount to apply a standard deviation. Moreover, the deviation within each individual measurement is significantly larger than the differences between the averages of the measurements. Therefore, the average of the deviations seems an appropriate value for the total error.

Chapter 5

Results

The results are presented in different representations. The deposit thickness is firstly presented according to Pouliquen [1]. Second, the same data is used to determine a critical diameter. The particles are ranked to their basal friction and the differences in flow regimes are discussed. Further, additional results for the influence on the deposit of chosen parameters like sample mass and slit height are included. Finally, pictures of each deposit are added to give a visual representation of the experiments. On the basis of these pictures, an elaboration on the deposit length and shape is given.

5.1 Basal friction

The basal friction of the monodisperse samples is analysed on the basis of the deposit thickness h_{stop}. The sensitivity of this thickness for changes in the used amount of particles or the slit height of the gate are studied as well. Finally the uniformity of the deposit thickness is studied by measuring the deposit at several positions.

5.1.1 H_{stop} data representation

The results for the h_{stop} measurements are presented in Figures 5.1(a) and 5.1(b). The dimensionless results follow from the non-dimensionless results by deviding them with the average particle diameter. This average diameter is assumed to be the average of the largest and smallest particle size of the sample.

The dimensionless results give a better insight in the behaviour of the particles, since it is a relative thickness compared to the diameter of the particles itself. For example, in figure 5.1(a) at 27° the thickness for the 1.00 - 1.3 mm and 0.15 - 0.25 mm samples is about the same. The deposit of the 1.00 - 1.3 mm particles is considered thin, because only a two particle thick layer stays on the plane, whereas the 0.15 - 0.25 mm deposit is considered thick, because an approximately 10 particle thick deposit stays on the plane.

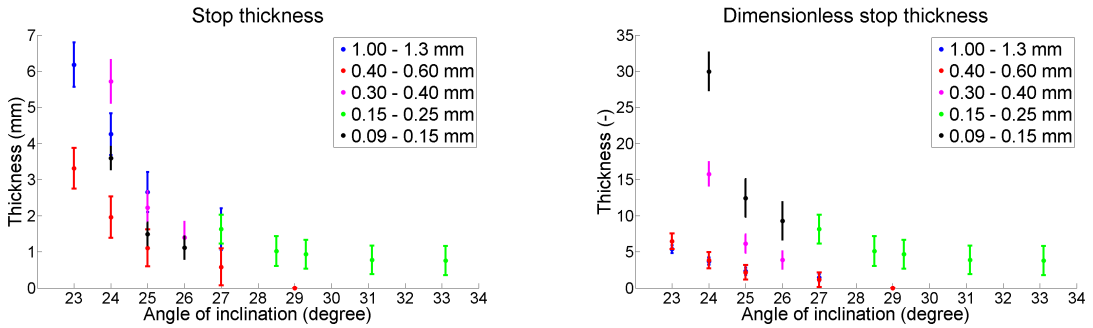

(a) Results h_{stop}

(b) Dimensionless results h_{stop}

Figure 5.1: Results h_{stop}

Too little data points are available to plot the mathematically correct curves according to Pouliquen [1], because in order to fit the data properly at least θ_1 and θ_2 should be known.

Only for the 0.40 - 0.60 mm sample θ_2 and θ_1 can be roughly estimated. In spite of the amount of data points, the trend of all experimental data points is likely to be compatible with a fit of the mathematical model. This resemblance can be used to roughly approximate the outcome of not performed experiments.

5.1.2 D_c data representation

In order to predict the behaviour of the bidisperse samples, the critical diameter is determined using the h_{stop} measurements. Figure 5.2 shows the critical diameter, measured at inclinations of 24° and 25°. For both inclinations the particles with an average diameter of 0.20 mm no flow occurred, so the thickness could be interpreted as infinite. For reasons of convenience a thickness of 50 is displayed in the graph in figure 5.2.

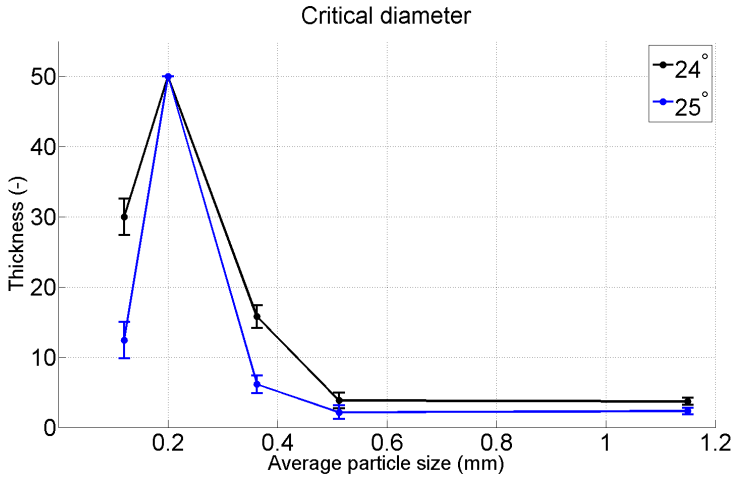

Figure 5.2: Results represented to show critical diameter

The 0.15 - 0.25 mm sample is the sample with a critical diameter, since a peak in the deposit thickness occurs. All samples with larger and smaller diameters have smaller thicknesses and therefore a smaller basal friction.

5.1.3 Order samples according to basal friction

The ballotini samples can be ranked in terms of basal friction, μ_b, for each inclination using the data presented in figure 5.1(b). In case of the 0.40 - 0.60 mm and 1.00 - 1.3 mm samples it is disputable which sample has the highest friction, since the deposits thicknesses are very close together and the result for the 1.00 - 1.3 mm is always within the measurement error of the 0.40 - 0.60 mm. Ignoring the error bars, the data can be split into two rankings, as shown in figure 5.3. In the Discussion section of this report the choice to ignore the error bars is discussed.

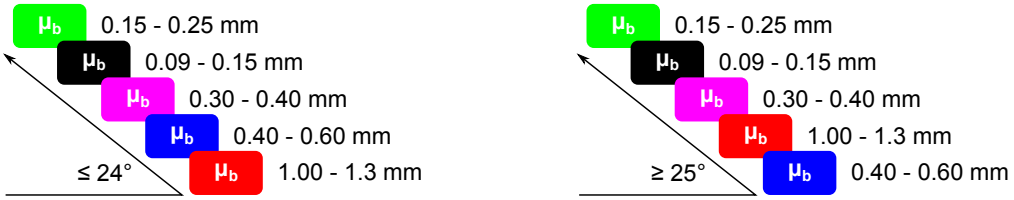

(a) 24 (b) 25

Figure 5.3: Friction ranking

5.1.4 Flow regimes

The data points of the 0.15 - 0.25 mm sample are in a different area of the graph than all the other data points. The smallest angle ($\theta_1 = 27°$) at which the 0.15 - 0.25 mm starts to move is only slightly smaller than the presumable θ_2 (29°) for the 0.40 - 0.60 mm ballotini. Apart from the different angles at which the 0.15 - 0.25 mm flows, the flow behaviour also looks different from the other particle flows. At these high angles, the beads come down in 'waves' instead of one front propagating down the slope. A schematic drawing of the different types of propagating flows is given in figure 5.4.

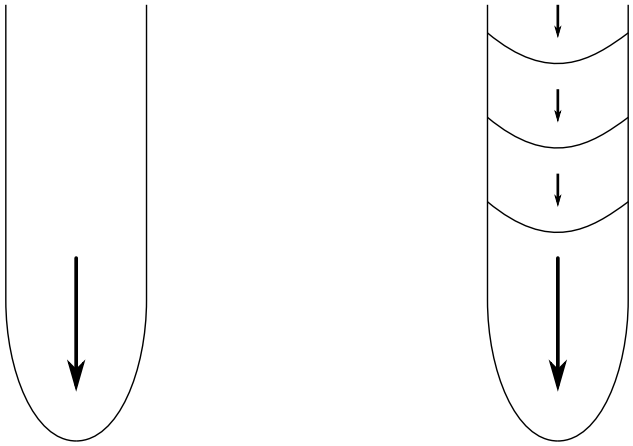

(a) A single front propagating downstream, observed for all samples except the 0.15 - 0.25 mm

(b) A large front propagating downstream, followed by several 'waves' of smaller flow fronts, only observed for the 0.15 - 0.25 mm particles

Figure 5.4: Schematic comparison between flow regimes

5.1.5 Influence of the slit height on h_{stop}

The experiments in order to determine h_{stop} are all performed with slit heights of 1.0 cm. The results obtained in these experiments are checked for their sensitivity to varying slit heights. Additional experiments with three different samples at three different inclinations are carried out. Figure 5.5 shows the results for the three different experiments.
The large errorbars prevent drawing a clear picture of the sensitivity of the results to the slit height. Neglecting these errorbars, in each case a small change in h_{stop} occurs with changing the slit height. The change is relatively small compared to the particle diameter and even smaller in terms of the total deposit thickness. The largest change in terms of particle diameter is an increase of deposit of about $^1/_4$ the diameter for the 0.30 - 0.40 mm sample. The largest change in terms of total deposit thickness is a decrease of about 10% for the 1.00 - 1.3 mm sample.

5.1.6 Influence of the mass on h_{stop}

Not all experiments are performed with the same amount, measured as mass, of particles. additional experiments are performed with varying masses to justify this choice. Two different samples are tested with two different mass alterations at three different angles, as shown in figure 5.6.
The influence of varying the mass seems relatively small for the experiments at 24° and 25°. The result for the runs at 27°shows a relatively large influence on the deposit thickness. The change

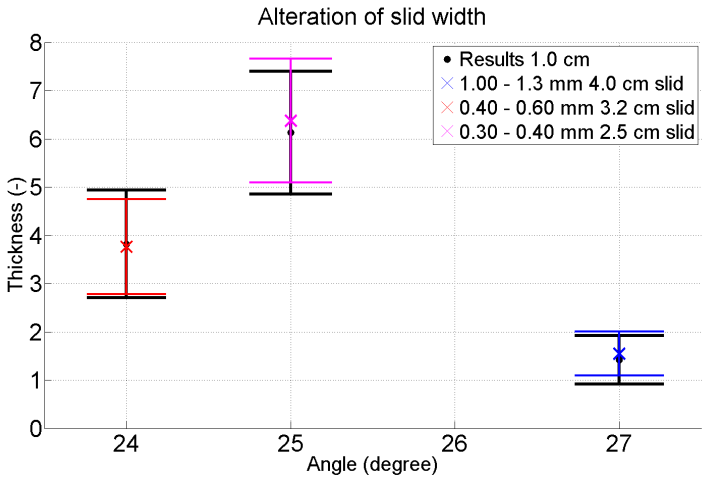

Figure 5.5: Results for varying slit height

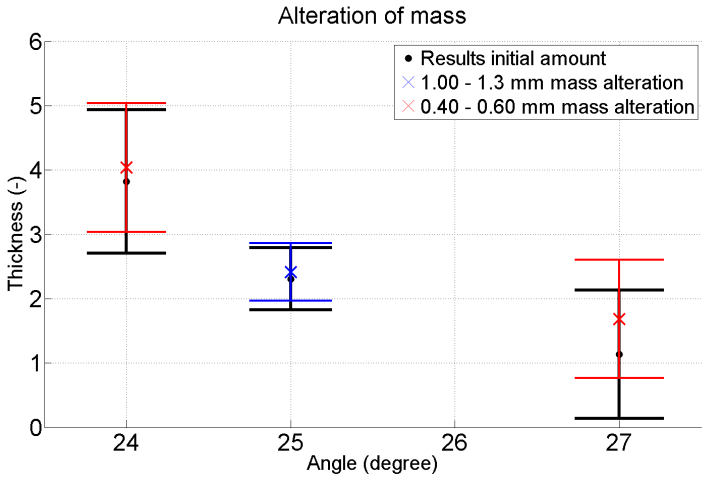

Figure 5.6: Results for varying mass

is about $^1/_2$ the particle diameter and an increase of about 50% of the total deposit thickness. Nonetheless, this effect could be attributed to the measurement position if the thickness of the short deposit is measured close to the front of the flow. The results at 24° and 27° are obtained with the same particle samples and the same mass ratio between the different experiments.

5.1.7 Effect of the position of the laser scanner on the measured thickness

The position of the laser scanner for most experiments is at a distance of 500 mm downslope from the home position. The home position is at around 30 cm distance from the compartment. To check whether or not the measurements at this position are representable for the complete deposit the thickness of several deposits is measured at different positions, see figure 5.7. The 0.40 - 0.60 mm sample is used for all measurements, but the inclination of the chute or the amount of ballotini change.

The data points in figure 5.7(a) and 5.7(c) are close together which suggest the thickness is independent of the position. The only outlying data point is the -1200 mm measurement in figure 5.7(b). The position of the laser scanner was shifted from -1500 mm to -1200 mm to do the measurement, since the deposit did not reach the -1500 mm position. The measurement at -1200 mm is positioned at the front of the deposit, which is not a representable location to measure the thickness.

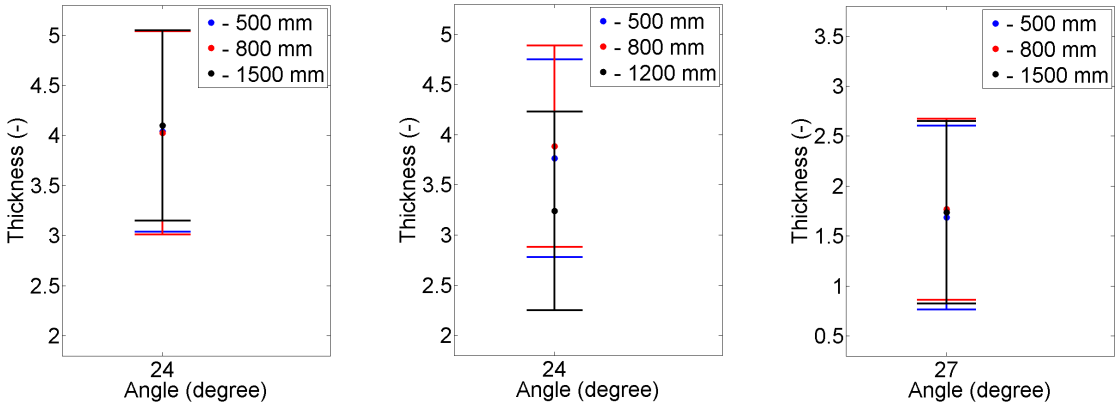

(a) 4.30 kg (b) 1.60 kg (c) 1.60 kg

Figure 5.7: Effect of laser scanner position for 0.40 - 0.60 mm ballotini with 1.0 cm slit

5.2 Increased mobility and instabilities in bidisperse flows

After mapping the behaviour of the samples in combination with the rough base, one inclination is chosen for further investigation. Since θ_1 of the 0.15 - 0.25 mm sample is too high in comparison with the θ_2 of the other samples, the 0.15 - 0.25 mm particles are excluded from further investigations.The angle is chosen such that, even with an increased mobility in case of bidisperse samples, there always is a deposit left on the chute for both sizes. The inclination is therefore set at 25°.

Figures 5.8 and 5.9 show the deposits of all the experiments. On top of each picture of a deposit the runout length is projected. On the left side is the average of the three lengths projected and marked with a dashed line.

Each monodisperse deposit has about the same shape and length (figure 5.8). The length is the main differentiator, since the width of all the different deposits is about the same. The deviation in length within the 0.09 - 0.15 mm measurements is the largest; the shortest length is 145 cm and the largest 155 cm. The differences between the shortest and longest deposit for the 1.00 - 1.3 mm, 0.40 - 0.60 mm and 0.30 - 0.40 mm are 1 cm, 3 cm and 2 cm respectively. In no case outliers occur either in length or in shape.

The runout length of the bidisperse mixtures (figure 5.9) differs more in length than for the monodisperse samples (figure 5.8). The variance in the length of the 1.00 - 1.3 mm / 0.40 - 0.60 mm mixture is the largest, for the shortest and longest deposit vary more than 52 cm. One of the flows ran of the chute, so an exact deposit length could not be determined. In that case, the length of the chute, 260 cm, is used to determine the average run out length. The other two mixtures have significantly shorter deposits with a smaller variance and a more uniformly shaped.

The differences in shape are caused by instabilities, known as fingering, and are most dominantly present in the 1.00 - 1.3 mm / 0.40 - 0.60 mm mixture. In the other two samples only in one of the three experiments a small finger occurred. In the third picture of figure 5.9(c) at the tip of the deposit the red part splits in two. In the first photo in figure 5.9(d) a small part of both particle deposits form a small finger. Subsequently, figure 5.9(e) shows a close up of this finger. The fingers seems to occur from a second flow where the small red particles form levees on the side and the interior consists of the large white particles. This is an unexpected inversion of the flowing patterns and to the authors knowledge not described in literature.

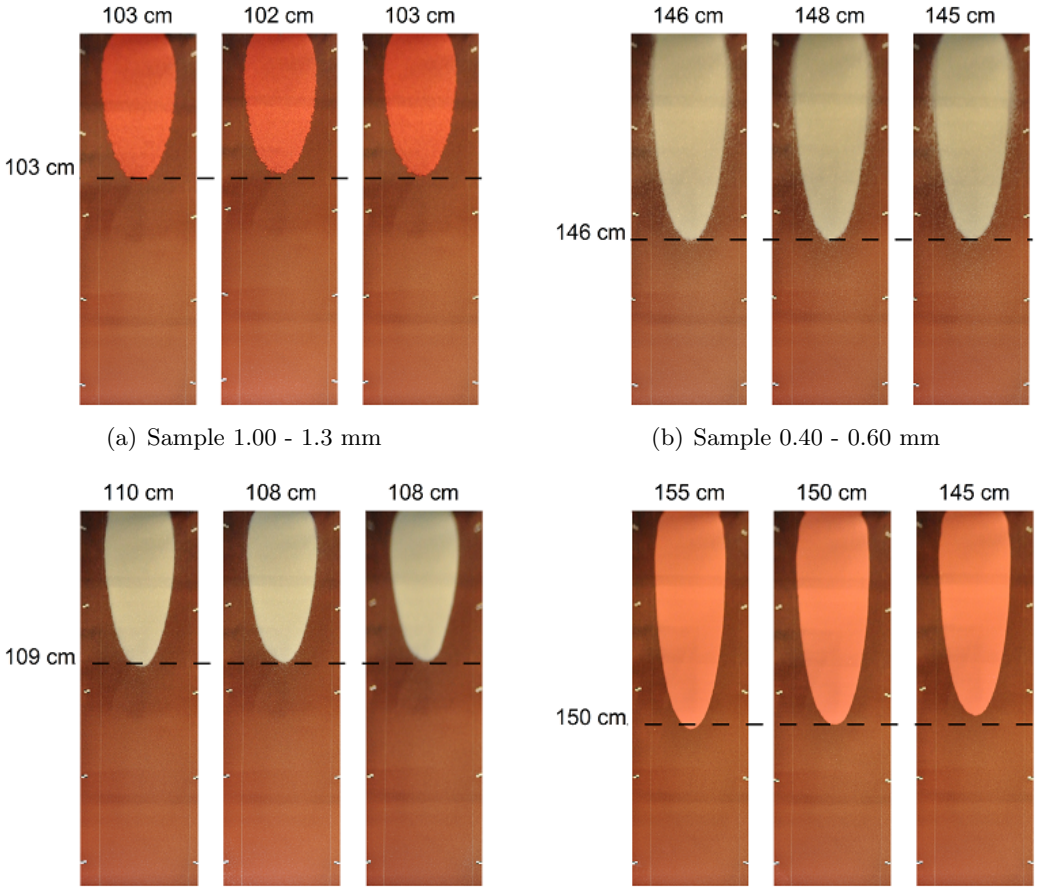

(a) Sample 1.00 - 1.3 mm

(b) Sample 0.40 - 0.60 mm

(c) Sample 0.30 - 0.40 mm

(d) Sample 0.09 - 0.15 mm

Figure 5.8: Deposits of the monodisperse flows

The length of the 1.00 - 1.3 mm / 0.40 - 0.60 mm mixture (figure 5.9(a)) is increased significantly compared to both monodisperse deposits (figure 5.8(a) and 5.8(b)) and the 1.00 - 1.3 mm / 0.30 - 0.40 mm mixture shows a slightly in length increased deposit (figure 5.9(b) compared with Figures 5.8(a) and 5.8(c)). The third mixture, 0.40 - 0.60 mm / 0.09 - 0.15 mm, has a slightly increased length, but is close to the deposit length of the small particles (figure 5.9(c) compared with 5.8(c) and 5.8(d)). The monodisperse deposit lengths of the 0.40 - 0.60 mm and the 0.09 - 0.15 mm are close together (figure 5.8(b) and 5.8(d)). The bidisperse runout of these two ballotini sizes vary not much from the monodisperse deposit (figure 5.9(d)).

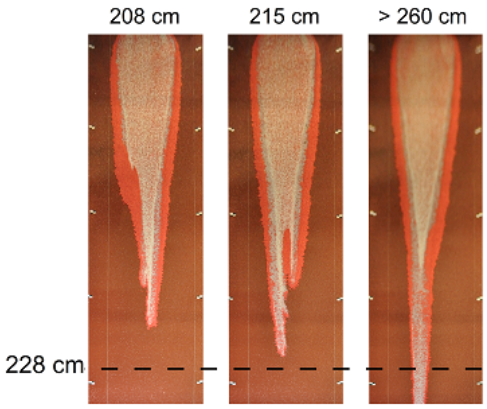

(a) Mixture 1.00 - 1.3 mm / 0.40 - 0.60 mm

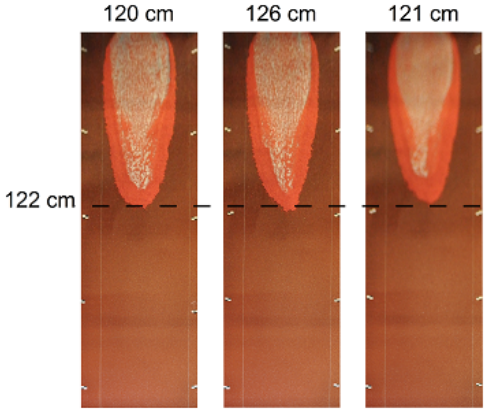

(b) Mixture 1.00 - 1.3 mm / 0.30 - 0.40 mm

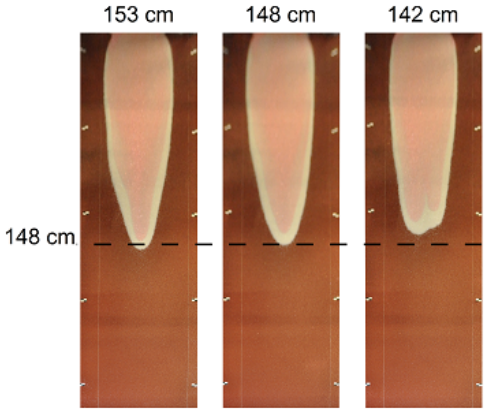

(c) Mixture 0.30 - 0.40 mm / 0.09 - 0.15 mm

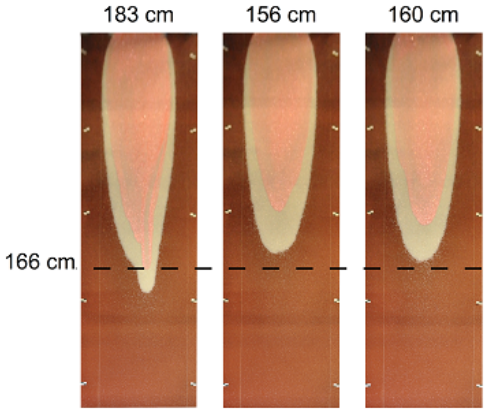

(d) Mixture 0.40 .0.60 mm / 0.09 - 0.15 mm

(e) Close up of the figure emerging in the 0.40 - 0.60 mm / 0.09 - 0.15 mm mixture

Figure 5.9: Deposits of the bidisperse flows

Chapter 6

Discussion

6.1 Analysing laser scanner data

The data plots do not correspond with the actual measured surface and do not meet the accuracy of the laser scanner specifications. Even when measuring a flat, smooth surface the data plot shows arcs, as if the surface were curved. Moreover, several arcs appear, with a certain spacing between each other. This spacing is about 0.2 mm, which is about the same order of magnitude as the expected deposit thicknesses. Since several arcs occur, the overall deviation in most measurements is around 0.5 mm. The accuracy claimed by the specifications of the laser scanner is 40 μm. A more detailed description of the arc pattern in the data, the specifications of the laser scanner and the calibration data is included in Appendix A.

The variance within the data is too big to say something with certainty about the actual deposit thicknesses and the sensitivity to altering settings. Especially for the smaller particle sizes a deviation of 0.5 mm is inaccurate, for the possible range of the result is almost 10 particle diameters. For studying the trends in figure 5.1 an accurate measurement is not essential, but when several h_{stop} thicknesses are close together it is hard to determine which has the higher basal friction. In order to predict the behaviour of bidisperse mixtures at any angle this is essential.

In some cases the high error is neglected to study the results in more detail. In every plot of the laser scanner data, a certain pattern appears. When several measurements are plotted in the same figure, the patterns of the different files fit as if it was one measurement. Most likely this pattern causes the high deviation within the measurement. Since all the files have the exact same pattern, and therefore deviation, it is assumed that the measurements relative to each other have a much smaller error. The absolute thicknesses of the deposits remain uncertain.

6.2 Measurement procedure and use of the equipment

The accuracy of the measurement of the deposit could be increased by measuring a deposit at different positions on the deposit. Eventhough the measurements taken at several locations show only minor differences over the length of the deposit, it may be useful to do a swipe measurement over a larger area of the deposit to increase accuracy. Additionally, a swipe measurement also provides information about trends in the height of the deposit along the runout.

The polystyrene inserts to decrease the size of the compartments are not ideal to perform reliable research. Firstly, the polystyrene material is easily damaged resulting in small polystyrene parts polluting the ballotini sample. Secondly, the ballotini stick to the polystyrene walls. These remaining beads in the compartment are not recorded and therefore decreases the reliability of any comparisons between different runs. This problem is solved by covering the polystyrene with paper. Finally, the inserts do not close off the limited compartment properly. In some cases ballotini slip underneath the inserts and are not released. Another area which is not closed properly is the space between the set of gates. The polystyrene inserts only reduce the compartment up to the gate which remains static. After this barrier the beads are free to spread over the full width of the compartment. Some additional inserts underneath the static gate reduce the

spreading highly, but do not prevent leaking completely.

The mixing procedure is likely to affect instabilities. The only applied method in this study is stirring the material before pouring it in the reservoir. This is a quick but not very precise method, because the two phases of material are not necessarily evenly distributed. In some flows an accumulation of particles at one side of the front causes an asymmetric or even unstable flow. If the instabilities could be assigned to the used mixing procedure, could be investigated by changing the initial state with a well controlled process. Goujon et al. [2] state that if the initial state is a layered mixture of the two phases the instability of the flow decreases.

The best way to assure every experiment is conducted at the same angle is to not move the inclinometer. Unfortunately, this is not always possible, since other people in the lab borrow it from the chute. The position where it is currently located, between the frame, is fairly reliable because any small changes with respect to the previous position does not result in a deviation larger than 0.1°, which is the accuracy of the inclinometer. Large changes are easy to prevent at this position, for the inclinometer is aligned with the frame. If the angle of the chute has to be determined very precisely, the difference between the angle of the setup location of the inclinometer on the frame and the actual angle of the chute should be known.

The distribution of the particle diameters within a sample has to be known to calculate the average diameter. Using the value in the middle between the maximum and minimum diameter of the sample is a fair assumption, but does not necessarily have to be true. The distribution of the diameter can be skewed for several reasons. It is possible the particles are provided with a skewed diameter distribution. Another possibility is that on one side of the sample the sieving is more accurate than on the other side. This imbalanced sieving leads too either more large or small particles in the sample and thus a skewed distribution.

6.3 Results of the experiments

So far, the shape of the particles has not been taken into account, since they were assumed to be perfectly round. However, as shown in the pictures in figure 4.3, not all particles are spherically shaped. Especially the 0.15 - 0.25 mm particles are oddly shaped. Likely, these odd shapes increase the basal friction and cause the behaviour of this sample incomparable to the other samples. The other samples are fairly well shaped with only a few non-circular shapes. In none of these samples any angular particles exist. Since the results for the 1.00 - 1.3 mm and 0.40 - 0.60 mm samples are very close together the particle shape could influence the ordering of the samples (section 4.1.3). When both samples have the exact same shape it is possible the 0.40 - 0.60 mm also has a lower basal friction than the 1.00 - 1.3 mm at angles smaller than 24°.

Three experiments are not sufficient to determine if results may be outliers. Statistically it is really hard to say anything about the distribution of measured data if only three data points are available. In addition, the bidisperse samples were merely tested at the angle of 25°and in 50 - 50 % mixtures of small and large particles. Changing these configurations may affect instability and mobility of the flow, due to changing frictional behaviour. Hence, all conclusions drawn in this report for bidisperse flows in general should be justified with additional experiments at varying angles and varying mixing ratios. Nonetheless, the number of conducted experiments serves the purpose of this research well, since insight in the behaviour of the available particles in the lab is expanded in the limited time available.

A significant amount of 1.00 - 1.3 mm ballotini bounces down the chute not depositing. After

one of the experiments with a 0.30 - 0.40 mm / 1.00 - 1.3 mm mixture the amount of ballotini that was cleaned from the chute was weighted. The difference between the initial mass and the mass after depositing and cleaning of the 0.30 - 0.40 mm ballotini was less than 10 g whereas this difference for the 1.00 - 1.3 mm ballotini was more than 150 g. Since significantly less ballotini deposits, in comparison the length of the deposit is likely to be shorter. If the bouncing of the ballotini also affects the thickness of the deposit is hard to tell: the interior part looks not affected by this behaviour, since most particles start bouncing from the sides and front of the flow. Therefore the thickness of the deposit may also not be affected.

The phenomenon of roll waves, in this investigation observed for the 0.15 - 0.25 mm sample, is earlier observed and studied by Félix et al. [5], Takagi et al. [7] and Forterre & Pouliquen [22]. In their studies they show that roll waves occur at high inclinations, which is in agreement with the observations in this study. However, the 0.15 - 0.25 mm sample does not flow at all at low inclinations ($\theta \leq 26°$) and immediately shows roll waves at any larger inclination. The absence of a steady flow is not covered in previous studies [5, 7, 22] and does not fit within the scope of this research, but could be an interesting topic to investigate further.

All bidisperse mixtures were expected to show an increased mobility compared to their monodisperse deposits. Nevertheless, in two mixed samples no increased length was determined. The deposit length seems to be determined by the deposit length of the beads with the lowest basal friction in the mixture e.g. the monodisperse 0.09 - 0.15 mm sample has a longer runout length than the monodisperse 0.30 - 0.40 mm sample, but is roughly of equal length as the 0.30 - 0.40 mm / 0.09 - 0.15 mm mixture. What's more, one of the 0.30 - 0.40 mm / 0.09 - 0.15 mm experiments shows a decreased runout length, likely due to the large accumulation of white particles at the front which restrain the red particles in flowing further.

The other two mixed samples show an increased length and in one case (1.00 - 1.3 mm / 0.40 - 0.60 mm mixture) this is likely caused by fingering. When a finger appears the width of the finger is significantly smaller than the total width of the flow and, assuming a constant h_{stop} over the total deposit, therefore means a significant increase in length. In the second case (1.00 - 1.3 mm / 0.30 - 0.40 mm mixture) it is uncertain if the total amount of deposited ballotini is comparable since the 1.00 - 1.3 mm ballotini tends to bounce off the chute. This effect seemed to be more significant in the monodisperse flows, but was not properly recorded. So if the deposit length of the mixture is longer due to the effect of increased mobility or the larger amount of depositing particles is uncertain.

It is striking that the monodisperse sample with the highest basal friction (0.09 - 0.15 mm) has the longest runout length even more so since Goujon et al. [3] determine d_c, and thus the basal friction, based on the absolute deposit length. The deposit length only relates to the absolute h_{stop}, because the volume of the sample remains constant during flow i.e. a thick non-dimensionless h_{stop} means a short deposit and vice versa. Comparing the samples on the basis of their absolute deposit thicknesses and deposit length confirms this statement. Nonetheless, relating the results of the order of basal friction magnitude to the occurrence of instabilities in this investigation seems to confirm the correctness of the use of the dimensionless h_{stop} for determining the basal friction and therefore eliminate the correctness of using of the deposit length.

Chapter 7

Conclusion

Granular flows comprise a variety of flow forms such as snow avalanches and transportation flows in industry. Any research into this phenomenon therefore has a wide range of applications. Nevertheless, performing experiments can be difficult due to a lack of reproducibility. This investigation is therefore aimed to gain understanding in the use of the particular experimental setup at the University of Cambridge based on the frictional behaviour of the particles. The first experiment determined the magnitude of the basal friction for different ballotini samples. The results were represented in terms of h_{stop} and d_c. The second experiment showed the behaviour of the mono- and bidisperse samples of ballotini.

The h_{stop} curves do not show any surprising results and follow the trend found by Pouliquen [1]. Even though the 0.15 - 0.25 mm particles behave differently from the other samples, they still seem to fit in the pattern. Experiments performed at higher angles would be needed to confirm this expectation, since a trend towards a 0 thickness deposit is not clearly visible.

The results show indeed the existence of d_c at $^1/_2$ the roughness, but differ slightly from the results shown by Goujon et al. [3] for particles larger than d_c. At an angle of 25°the basal friction of 1.00 - 1.3 mm is higher than the 0.40 - 0.60 mm basal friction, which does not correspond with the expectation that the basal friction decreases with particle size beyond d_c.

Altering either the slit height, mass of the sample, or position of the laser scanner seems to have no significant influence. In most cases the original measurement data and the altered measurement data are close together (within about 0.2 particle diameter) and in all cases within the error. Despite the high error, the results show that altering the settings of the setup does not affect the outcome of the study.

The behaviour of the mixed samples relates to their related monodisperse basal friction. The mixture where the large particles have a higher basal friction than the small particles becomes easily unstable. If the small particles have a larger basal friction the flow is stable. This behaviour is described earlier by Goujon et al. [2] and can be explained by the theory of Pouliquen & Vallance [19]: when the small particles, generally located in the center of the flow, have a lower basal friction than the large particles, the small particles overtake the front due to a higher flowing speed. When the small particles overtake the front a finger occurs.

Nonetheless, when no instabilities occur the flows do not show a significant increase in length, which contradicts the expectation of an increased mobility in any bidisperse mixture. The bidisperse deposit length is almost exactly equal to the longest associated monodisperse deposit length. A further investigation into this topic would be required to explain this behaviour.

Moreover, since the deposit length of the 0.09 - 0.15 mm ballotini sample is the longest, but is not the sample with the lowest basal friction the assumption to use the dimensionless thickness as a measure for the magnitude of the basal friction is justified. In other words, the absolute deposit thickness and therefore also the deposit length seem to be inadequate to determine the basal friction.

The cause of the fingers in the 0.30 - 0.40 mm / 0.09 - 0.15 mm and 0.40 - 0.60 mm / 0.09 - 0.15 mm mixtures is unclear. In this case several parameters could have influenced the stability of the flow. The mixing procedure could have affected the stability, since it determines the distribution of the different particles over the flow. Another cause could be pollution on the chute. Any material on the chute, such as small pieces of polystyrene, could influence the flow behaviour locally and cause fingers.

The results obtained in this study are relevant for future experiments for the following reasons. Firstly, insight in the flow behaviour based on basal friction saves the researcher time in setting up any bidisperse flow experiments. Secondly, unexpected behaviour was observed in some of the flows, which would be interesting to investigate in greater detail and is listed in Appendix D. Finally, the accuracy of the laser scanner now meets the specifications, owing to the alteration of the high resolution setting as a result of observations in this investigation of a too low accuracy in the laser scanner measurements.

Chapter 8

Personal reflection

This internship was one of the most valuable experiences of my academic education. It showed me I like doing research and as a result I am seriously considering applying for a PhD position. In this section I will reflect on my internship by highlighting my biggest competence improvements, some of my observations and the rewarding collaboration with my supervisor Dr. Vriend.

In my view, this internship enriched and improved my competences. Most of the aspects of performing research were taught in my study program, but I did not have the opportunities to practice them all extensively. Some of the aspects I was not very familiar with are literature review, performing experiments and data analysis. I still think I could read papers more critical and be more creative and accurate in analysing data, but I definitely made progress while practicing. Another great improvement is writing in English.

During this internship, I was highly motivated by the freedom I was given to discover the phenomenon of granular flows. I enjoyed searching for literature that would answer my questions and was maybe even more exited when I could not find answers. I found this learning process more rewarding than any course I have taken.

When I arrived in the Fluids group I had some trouble getting to know everybody just over the tea and lunch breaks. Especially the more senior people I found hard to reach out to. In any upcoming situation where I am the 'new person' I would try making a round trough the office on the first day, shortly introducing myself to everybody. I think this introduction round will make me feel more comfortable talking to people afterwards.

One of the big advantages of doing my internship at a university instead of a company were the many PhD students who were working in the same group. I really enjoyed meeting them during tea or lunch breaks. They definitely made my social life a lot easier and much more fun than it would have been at many companies.

Last but not least, I enjoyed working with my supervisor, Dr. Vriend. We did not meet very often, but the meetings were always very useful and motivating. Moreover, I always felt welcome to ask any question even without having a scheduled meeting. I appreciate she took my ideas seriously and we could discuss my work in an open discussion. It was a great pleasure to have Dr. Vriend as my supervisor and I look forward to working with her again.

Bibliography

[1] Pouliquen, O. Scaling laws in granular flows down rough inclined planes. Physics of Fluids 11, 542 (1999).

[2] Goujon, C., Dalloz - Dubrujeaud, B.& Thomas, N. Bidisperse granular avalanches on inclined planes: A rich variety of behaviors. European Physical Journal E 23, 199-215 (2007)

[3] Goujon, C., Thomas, N. & Dalloz-Dubrujeaud, B. Monodisperse dry granular flows on inclined planes: role of roughness. The European physical journal. E, Soft matter 11, 147-157 (2003).

[4] Bartelt, P., Glover, J., Feistl, T., Buhler, Y. & Buser, O. Formation of levees and en-echelon shear planes during snow avalanche run-out. Journal of Glaciology 58, 211 (2012)

[5] Félix, G. & Thomas, N. Relation between dry granular flow regimes and morphology of deposits: Formation of levees in pyroclastic deposits. Earth and Planetary Science Letters 221, 197-213 (2004).

[6] Deboeuf, S., Lajeunesse, E., Dauchot, O. & Andreotti, B. Flow rule, self-channelization, and levees in unconfined granular flows. Physical Review Letters 97, 158303 (2006).

[7] Takagi, D., McElwaine, J.N. & Huppert, E. Shallow granular flows. Physical Review E 83, 031306 (2011).

[8] Savage, S.B. & Lun, C.K.K. Particle size segregation in inclined chute flow of dry cohesionless granular solids. Journal of Fluid Mechanics 189, 311 (1988).

[9] Gray, J.M.N.T. & Ancey, C. Multi-component particle-size segregation in shallow granular avalanches. Journal of Fluid Mechanics 678, 535-588 (2011).

[10] Gray, J.M.N.T., Shearer, M. & Thornton, A.R. Time-dependent solutions for particle-size segregation in shallow granular avalanches. Proceedings of the Royal Society A 462, 947-972 (2006).

[11] Gray, J.M.N.T. & Chugunov, V.A. Particle-size segregation and diffusive remixing in shallow granular avalanches. Journal of Fluid Mechancis 569, 365-389 (2006).

[12] Gray, J.M.N.T. & Ancey, C. Segregation, recirculation and deposition of coarse particles near two-dimensional avalanche fronts. Journal of Fluid Mechanics 629, 387-423 (2009).

[13] Gray, J.M.N.T. & Kokelaar, B.P. Large particle segregation, transport and accumulation in granular free-surface flows. Journal of Fluid Mechanics 652, 105-137 (2010).

[14] Gray, J.M.N.T. & Thornton, A.R. A theory for particle size segregation in shallow granular free-surface flows. Proceedings of the Royal Society A 461, 1447-1473 (2005).

[15] Wiederseiner, S., Andreini, N., Épely-Chauvin, G., Moser, G., Monnereau, M., Gray, J.M.N.T. & Ancey, C. Experimental investigation into segregating granular flows down chutes. Physics of Fluids 23, 013301 (2011).

[16] Kokelaar, B., Graham, R., Gray, J.M.N.T. & Vallance, J.W. Fine-grained linings of leveed channels facilitate runout of granular flows. Earth an Planetary Science Letters 385, 172 (2014).

[17] Bartelt, P. & McArdell, B.W. Granulometric investigations of snow avalanches. Journal of Glaciology 55, 193 (2009)

[18] Johnson, C.G., Kokelaar, B.P., Iverson, R.M., Logan, M., Lahusen, R.G. & Gray, J.M.N.T. Grain-size segregation and levee formation in geophysical mass flows. Journal of Geophysical Research F: Earth Surface 117, (2012).

[19] Pouliquen, O. & Vallance, J.W. Segregation induced instabilities of granular fronts. Chaos 9, 621 (1999).

[20] Linares-Guerrero, E., Goujon, C. & Zenit, R. Increased mobility of bidisperse granular avalanches. Journal of Fluid Mechanics 593, (2007).

[21] Phillips, J.C., Hogg, A.J., Kerswell, R.R. & Thomas, N.H. Enhanced mobility of granular mixtures of fine and coarse particles. Earth and Planetary Science Letters 246, 466-480 (2006).

[22] Forterre, Y. & Pouliquen, O. Long-surface-wave instability in dense granular flows. Journal of Fluid Mechanics 486, 21-50 (2003).

Appendix A, Laser scanner

Measurement principle

An overview of the principle of the laser scanner is given in figure 8.1. The light source sends out a laser beam. When the light reaches a solid surface, it reflects and converges towards the receiver. On a CMOS array the laser line is replicated and evaluated in two dimensions.

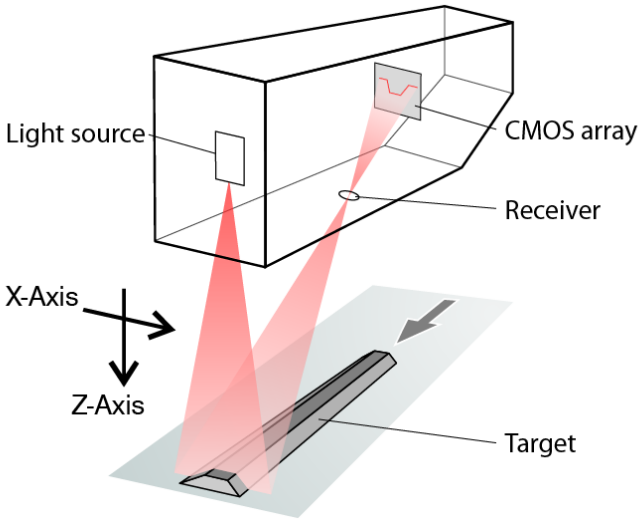

Figure 8.1: Measurement principle, from: Micro-Epsilon Instruction Manual

Data profiles

The data from the measurements taken with the laser scanner show a certain pattern. Figure 8.2(a) shows that, independent of the measured surface type, the data points are organized in curved layers. The curvature of the layers match with a perfect circle with a certain radius, as shown by the green arcs in figure 8.2(b). The arcs do not seem circular due to the scaling of the axis and the magnitude of their radius depends on the distance at which the surface is measured. In figure 8.2(c) the measurement distance is altered, but the radius of the plotted arc is kept constant with respect to the arcs in figure 8.2(a). If the measurement of the base is subtracted from a deposit measurement the arcs dissapear, as shown in figure 8.2(d). This method is in this investigation used in analysing the data.

The cause of this pattern has been unclear for a long time. In order to seek for a solution we contacted the manufacturer of the laser scanner, Micro Epsilon. The contact details are listed below. They suggested installing the program *scanCONTROL Configuration Tools*, which is a useful tool since it shows directly the effect of altered settings. Using this program, we saw that usually these patterns only appear with high threshold and/or low profile frequency. However, using our own code the patterns appeared for any threshold and any profile frequency. Eventually, we found that the option to use high resolution was switched off in our code and switching it on solved the problem.

Contact details:
Stefan Grüble: Stefan.Gruebl@micro-epsilon.de
Ulrich Eibauer: Ulrich.Eibauer@micro-epsilon.de

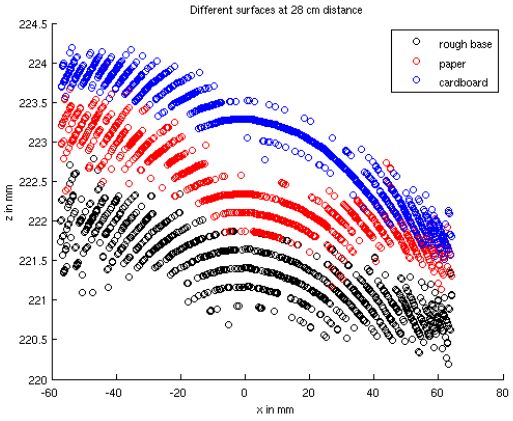

(a) Different surfaces at 28 cm distance from the laser scanner

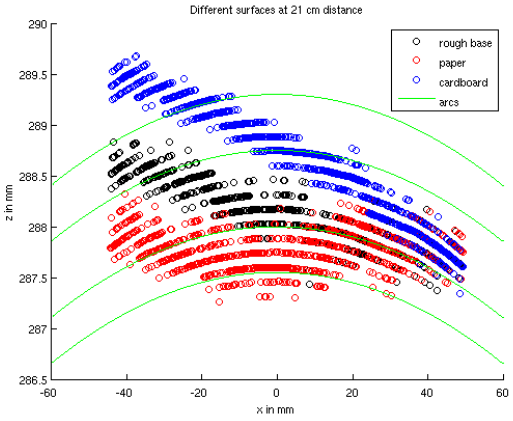

(b) Different surfaces at 21 cm distance from the laser scanner, with 4 arcs each with a radius of 288 mm

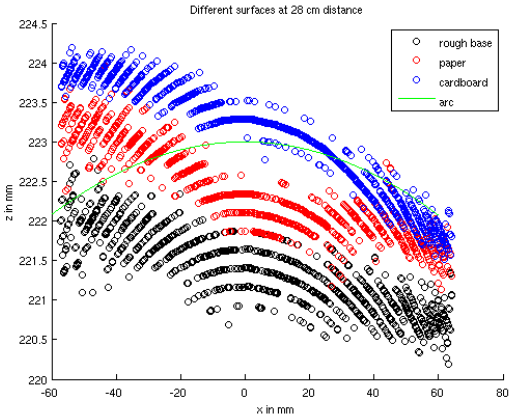

(c) Different surfaces at 28 cm distance from the laser scanner and an arc with a radius of 288 mm

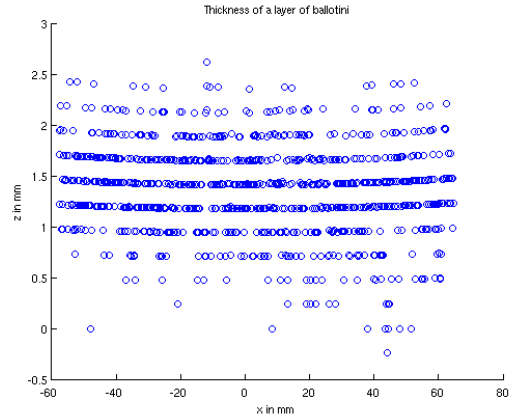

(d) Layer of ballotini, by subtracting a base measurement from the ballotini measurement

Figure 8.2: Data profiles

MICRO-EPSILON

Model		LLT2800-25		LLT2800-100	
Standard ranges, extended range in brackets (±5%)					
Measuring range z-axis		25 (55) mm	0.98" (2.17")	100 (245) mm	3.94" (9.65")
Start of measuring range (SMR)		62.5 (50) mm	2.46" (1.96")	145 (115) mm	5.71" (4.53")
Reference distance, midrange (MMR)		75 (82.5) mm	2.95" (3.25")	195 (235) mm	7.68" (9.25")
End of measuring range (EMR)		87.5 (105) mm	3.44" (4.13")	245 (360) mm	9.65" (14.17")
Resolution z-axis *		0.04%			
		10 µm		40 µm	
Linearity z-axis, ±3σ *		±0.2 %			
		±50 µm		±200 µm	
Measuring range x-axis	SMR	13 (23) mm	0.51" (0.91")	30 (50) mm	1.18" (1.97")
	EMR	18 (41) mm	0.70" (1.61")	50 (140) mm	1.97" (5.51")
Laser aperture angle		30 °			
Resolution x-axis		**256 / 512 points/profile (1024 points/profile)******			
Linearity x-axis, ±3σ *		±0.4 %			
		SMR 60 µm / EMR 80 µm		SMR 120 µm / EMR 200 µm	
Profile frequency		**to 1000 profiles/s**			
Measuring rate		**256,000 points/s**			
Light source		laser diode 655 nm, 15 mW			
Laser class		class 2M			
Laser off		remote - input and key switch			
Permissible ambient light (fluorescent light)		10,000 lx			
Protection class	sensor	IP 64			
	controller	IP 40			
Operating temperature		0...50 °C / 32...122 °F			
Storage temperature		-20...70 °C / -4...158 °F			
Weight	sensor	350 g		400 g	
	controller	3.5 kg			
Sensor cable standard length		2 m			
Output analog					
preprogrammed x- and z-axis, alternative profile parameter **		±10 V (16 bit, up to 150 kHz)			
Output/Input digital					
Interface (measurement data and control commands)		3x IEEE 1394 („FireWire"), 400 MBit/s (similar DCAM 1.30)			
		1x RS232 (115200 Baud)			
		1x RS422 (115200 Baud)			
Synchron-connector, input ***		sync-in, remote laser ON/OFF, mode			
Synchron-connector, output ***		sync-out, error, user mode (2x)			
Video signal (test and set up mode)		1 V_{SS} (BAS-signal, 8-bit-grey)			
Supply		24 VDC (±15 %) / 0.5 A			

All specifications apply for a diffusely reflecting matt white ceramic target - marginal position tolerance of the measuring-field is possible (sensor depending) SMR = Start Measuring Range EMR = End of Measuring Range

* for standard measuring ranges (512 points/profile preprogrammed)

** only for preprogrammed data, e.g. gap edge position, gap width, step heigth, angle

*** preprogrammed, other function possible

**** optional 1024 points/profile only in extended range

The laser unit of scanCONTROL 2800 uses a semiconductor laser with a wavelengh of 655 nm (visible/red) and 15 mW optical output (class 2M). The sensor is classified as laser class 2M. A warning sign is attached to the sensor housing.

MICRO-EPSILON

Sensor-Abnahmeprotokoll

LLT2800-100(009) v19-D2 S/N 09060295

Messung vom 19.12.2007 11:47:57
Protokoll vom 19.12.2007 11:56:03
Target Micro-Optronic-Standardtarget Matt-Metall
Version 1.36 (4.1)

ebenes Target, Neigung 5.302 Grad
globale Verschiebung 4.688 mm
Lagekorrektur dz/dx -0.132, dz/dz -0.231 Mikrometer/mm
Messpunkte insgesamt 534735, davon 92724 im Standardmessbereich

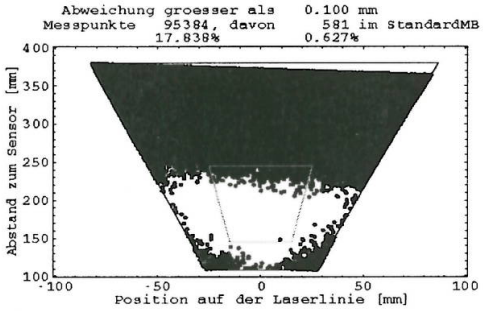

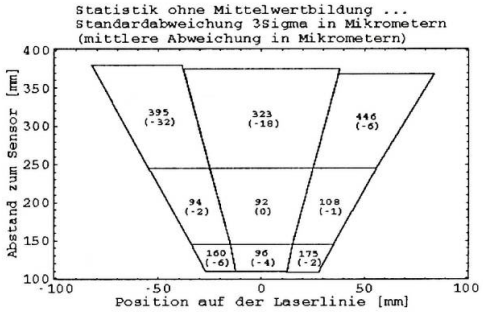

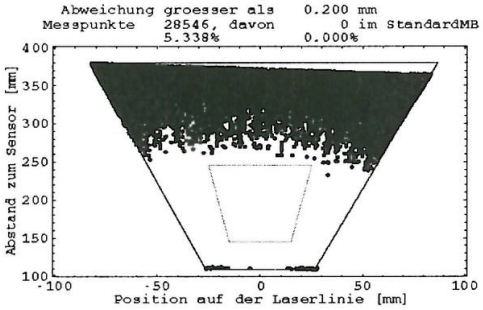

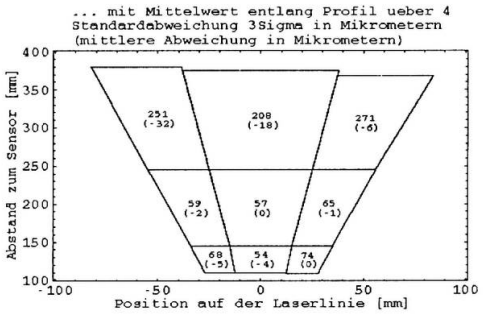

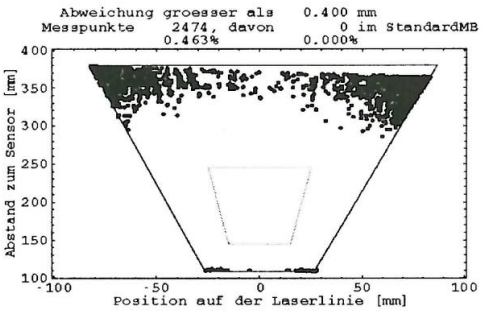

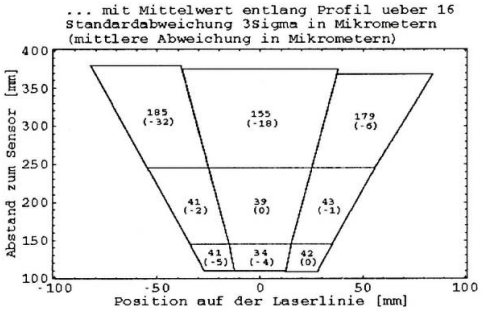

Appendix B, Experimental protocol

General instructions for performing an experiment

Preparing the chute

- Before using the chute, check if particles from previous experiments are cleaned up properly. There should be no particles left in the reservoir, on the chute and in the basin below the chute.
- It could be useful to also check between the two gates for particles. Particles tend to stick to the moving gate, but are hard to remove since the static gate has to be removed in order to access the moving gate. *Warning: always make sure the pressure is off when you are going to remove the static gate.*
- If necessary, remove all remaining particles from the setup. It might be useful to incline the chute first, in order to remove the particles more easily.
- Mount the static gate to the desired slit height.
- If required, reduce the size of the reservoir with the polystyrene inserts. Additional inserts can be used to avoid particles leaking between the two gates. Figure 8.3 on the following page shows the inserts covered with paper and with additional inserts attached to it.
- Set the chute to the desired angle according to the steps listed on the instruction sheet attached to the chute
- If necessary, install a camera on a tripod at the end of the chute. For easy reproduction mark the positions of the tripod legs with tape on the floor. A camera position as high as possible gives the best results.

Preparing a sample

- Make sure all the tins and cups you want to use are clear of particles.
- Weigh the desired amount of particles using the scale.

  Tip:Place the cup you want to use in one of the tins on the scale. This method will prevent particles from spilling all over the table or on the floor when you pour the particles into the cup.

If you are working with a monodisperse sample you can now move on to *Performing an experiment*. To finish preparing a bidisperse sample continue with the following steps:

- Weigh the desired amount of the second particle sample using the scale.
- Mix the two samples together in a cup or bowl by stirring for a brief period of time until the two particle phases are evenly spread. Figure 8.4 on the following page gives an example of the result after stirring.

Performing an experiment

- Pour the prepared sample in the reservoir.
- Even the particles with the chute i.e. use a flat piece of metal to move the top layer of particles upwards. Make this movement only once or twice, since it can influence the initial state of the sample such as packing fraction and mixture.

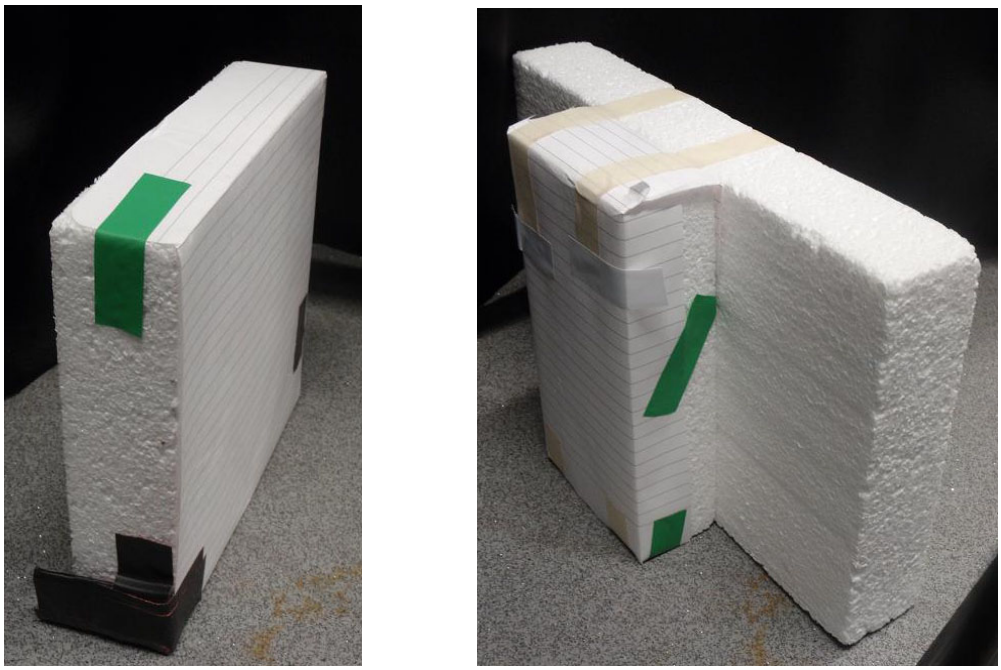

(a) (b)

Figure 8.3: Prepared polystyrene inserts

(a) Polystyrene side wall (b) Polystyrene back wall

Figure 8.4: Example of mixing result

- Open the gate.
- Wait till all particles are deposited. Take all the desired measurements.
- When all desired measurements are done, clean the chute from all ballotini and prepare a new sample. If you change to a sample with different ballotini, make sure you clean thoroughly in order to avoid the particles of the previous sample polluting the new sample.

Cleaning up

- Remove the polystyrene inserts from the reservoir.
- Thoroughly clean all ballotini from the chute with the appropriate brush and take extra

care clearing the reservoir of all particles. It may be advantageous to increase the inclination of the chute for easier cleaning. *Always make sure the chute is appropriately secured from falling down.*

- Empty the box in one of the large tins and use a brush to transfer as many particles as possible.
- Sweep the majority of ballotini from the basin with the appropriate dustpan and brush and add these particles to the other collected particles.
- Sweep the particles from the rails of the dead stops and add these as well to the earlier collected particles.
- Sieve all the ballotini and store them in the associated jars.
- Clean the table using the appropriate dustpan and brush.
- Sieve the collected particles from the previous step.
- Check the table for remaining particles and judge on the basis of the amount of particles if it useful to sieve again.
- Leave the table empty and clean for the next person.
- Sweep the floor around the chute (also underneath the anti-slip mat) and clean up the majority of particles using the appropriate dustpan and brush.
- Hoover the last few particles from the basin, box and dead stop rails. Be careful using the hoover since it can cause scratches on the surface which as a consequence makes it harder to clean again.
- Hoover the floor around the chute (also underneath the anti-slip mat).
- Lower the chute to the flat position according to the steps listed on the instruction sheet attached to the chute.
- Remove the static gate from the setup. *Warning: make sure the pressure is off before removing the static gate.*
- Clean the gates with a fine brush.
- Carefully hoover the ballotini from the reservoir. *Make sure to not touch the base, since you can damage the sand paper and therefore alter the roughness.*
- Reinstall the static gate.

Additional remarks

- Tie long hair back in order to avoid pollution of the samples.
- All particles that did not touch the floor can be reused.
- The screws of the moving gate tend to get loose a bit over time, which results in them scratching over the static gate. If you start to hear scratching noises, remove the static gate *(think about turning off the air pressure)* and tighten the screws.
- If you used the 0.09 - 0.15 mm ballotini, take extra care cleaning the setup, for it sticks to anything (walls, frame, brush etc.) It may even be useful to leave the chute at a steep inclination overnight, letting the particles come down the chute themselves.
- When you are planning the experiments take the particle size into account in determining the sequence. If, for example, you run an experiment using the 0.09 - 0.15 mm followed by an experiment with the 0.15 - 0.25 mm ballotini, the 0.15 - 0.25 mm is likely to get polluted with the 0.09 - 0.15 mm particles even if the chute is cleaned thoroughly. Due to the proximity of the sizes of the ballotini the pollution is not easily sieved out, if not impossible. Therefore, make sure subsequent samples can always be separated by sieving.

- The checked squares, handy for post processing pictures, are easily attached to the chute using double sided tape. The disadvantage is that if ballotini slips underneath they get loose and have to be reattached.

Specific settings for the basal friction experiments

Some of the setup properties vary for the different samples. The size of the reservoir is the same for all the experiments; 10 cm in width and 20 cm in length. The extra space from the barrier to the gate, is not taken into account. The slit height is set to 1.0 cm for all experiments. The amount of used ballotini differs for each set of experiments, Table 8.1. The position of the laser scanner is identical for most of the experiments, except for the 0.40 - 0.60 runs, Table 8.1.

The position was altered, because not all flows reached the distance where the laser scanner was mounted initially (- 800 mm). The amount of ballotini changes for the different experiments since, after the 0.40 - 0.60 mm experiments were performed the amount of already sieved 0.15 - 0.25 mm ballotini was limited. The same holds for the 0.09 - 0.15 mm experiments with 1.9 kg. The 0.30 - 0.40 mm and 1.00 - 1.3 mm samples were adjusted to the limitations of the 0.09 - 0.15 mm sample.

The sensitivity of h_{stop} for alterations in the experimental setup is investigated by carrying out additional measurements. The first experiment is changing the mass, Table 8.2. Subsequently, Table 8.3 gives information on the changes of the slit height. Finally, the effect of the measurement position is investigated by measuring a deposit at three different positions, given in Table 8.4. The angles and amounts are selected such that a relatively thick as well as a relatively thin deposit are measured.

Size	**Amount**	**Scan position**
0.09 - 0.15 mm	1.90 kg	- 500 mm
0.15 - 0.25 mm	2.50 kg	- 500 mm
0.30 - 0.40 mm	2.00 kg	- 500 mm
0.40 - 0.60 mm	4.30 kg	- 800 mm
1.00 - 1.3 mm	2.00 kg	- 500 mm

Table 8.1: Size specific settings

Size	**Inclination**	**Initial amount**	**Altered amount**
0.40 - 0.60 mm	24.0°	1.60 kg	4.30 kg
	27.0°	4.30 kg	1.60 kg
1.00 - 1.3 mm	25.0°	2.00 kg	5.90 kg

Table 8.2: Alteration of mass

Size	**Inclination**	**Initial slit height**	**Altered slit height**
0.30 - 0.40 mm	25.0°	1.0 cm	2.5 cm
0.40- 0.60 mm	24.0°	1.0 cm	3.2 cm
1.00 - 1.3 mm	27.0 °	1.0 cm	4.0 cm

Table 8.3: Alteration of slit height

Inclination	**Amount**	**Positions**
24 °	4.30 kg	- 500 mm
		- 800 mm
		- 1500 mm
24 °	1.60 kg	- 500 mm
		- 800 mm
		- 1200 mm
27 °	1.60 kg	- 500 mm
		- 800 mm
		- 1500 mm

Table 8.4: Alteration of the measurement position, performed with 0.40 - 0.60 mm ballotini and 1.0 cm slit height

Appendix C, Levee formation proposal

This research proposal is a first draft and can never be used as a functional proposal. It could be used as inspiration for setting up a research into the formation of levees.

Research Questions

In which ways does particle size influence the formation of levees?

- How do levees develop over time?

  Look levees at the static front the same as the moving front levees further upstream?
- How does levee occurring in flow of 2 different size particles differ from levees of uniform size flow?
- In what way does the magnitude of differences between size influence the formation of levees?
- How does the development/outcome of a levee alter with altering mixture of ballotini?
- Does initial state matter (which size on top)?
- If difference in size is larger, earlier developed levees?

Hypothesis

It is expected particle size influences the formation of levees in several ways.
First, it is expected that with increasing size difference, size segregation is becoming easier. For the formation of levees this probably means, that the levee develops faster over time. If the levee is not influenced by size segregation, it is expected the remaining flow along the levee only provides shear. Sharpened levees, as found by Kokelaar et al. [16] are expected to arise.

Second, the influence of size segregation on the formation of levees is believed to fortify the process. Where levees in monodisperse flows only occur when the channel is emptied [5], in polydisperse flows it is expected to occur immediately with segregation.

Third, the formation of levees is expected to always develop in the same way, independent of particle size or position in the flow. However, it could be levees in the final deposition are in different stages of the forming process and therefore differ from each other.

Last, the initial state of the ballotini is believed to be of neglectable influence. It is likely, that during the first collapse particles are partly mixed again. If any influence would be noticeable, it is in the time domain of the formation, because it might take longer, or shorter, to fully segregate.

Setup

A compartment on top of a 3 meter long chute will be filled with a mix of ballotini (figure 8.5). The compartment bottom size is 150 x 100 mm. The original compartment size is about 300 x 300 mm, so blocks of polystyrene are used to decrease the volume. The amount of ballotini will be 1,6 kg, which corresponds to about 1 liter. The amount of ballotini and the size of the compartment were determined in preparatory research. To prevent a very chaotic collapse once the

gate is opened, an extra barrier is added. A metal plate will be mounted between the ballotini and the gate, leaving an opening of 1-4 cm. The opening allows a more regulated collapse, but does not influence the flux such that a steady state will occur. The angle of the chute is chosen to be within 24 - 25 degrees, also based on preparatory research. The roughness of the chute is 425 μm.

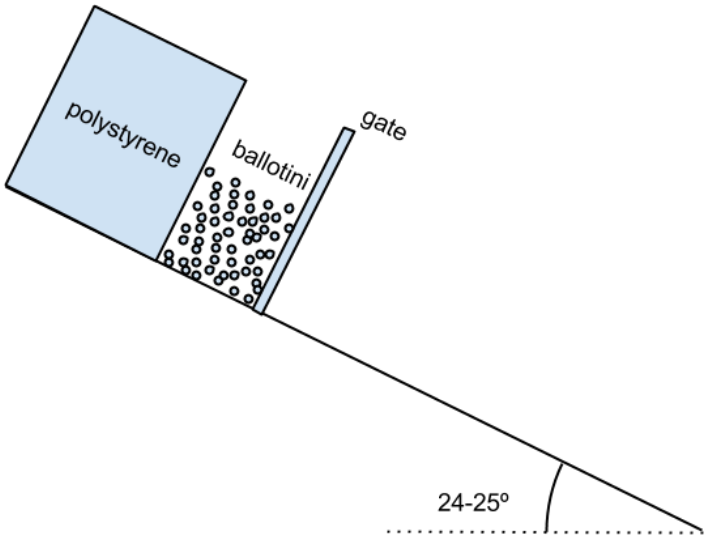

Figure 8.5: Proposed setup

Since size segregation is the main feature of this research, two different sizes of ballotini will be used in each setup. Initially, the ballotini will be poured into the compartment in a random distribution. The poured ballotini is initially distributed unevenly. A small piece of flat metal is used to flatten the surface with the angle of the chute, as shown in figure 8.6.

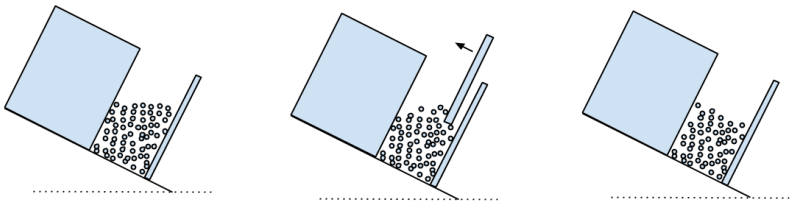

Figure 8.6: Flattening procedure

In order to study the influence of different particle sizes, several configurations will be studied. Table 8.5 shows the proposed configurations. All experiments will be performed with an equal amount of two different sizes of ballotini.

If interesting differences arise between the use of the relatively big (configuration 1) ballotini and small (configuration 3) ballotini, it is possible to expand the experiments with a new configuration. Ballotini of 0.50 - 0.75 mm is available, but will initially not be used. If more configurations are needed with smaller step sizes, it is possible to add it to the setup.

Configuration no.	Big size	Small size
1	1.00 - 1.3 mm (red)	0.40 - 0.60 mm (white)
2	1.00 - 1.3 mm (red)	0.15 - 0.25 mm (white)
3	0.30 - 0.40 mm (white)	0.09 - 0.15 mm (red)

Table 8.5: Configuration of mixing samples

Once the ballotini is positioned in the compartment, the gate will be released and the ballotini will flow down. During the flow of the ballotini, a laser scanner will collect data of the development of the height and width of the levees. For this purpose the scanner is fixed at one position, while the ballotini flows past it (Eulerian setup). After the ballotini deposited, the laser scanner is used to scan the levee over the full length of the deposit (figure 8.7(a)). Since the speed of the laser scanner is very slow compared to the shutter time, the movement is believed to be of neglectable influence. Another important feature is the particle size used in the experiment. The order of movement during shutter time should be about the order of the biggest particles used. This idea is applied to ensure a certain speed of the measurement, without losing too much accuracy.

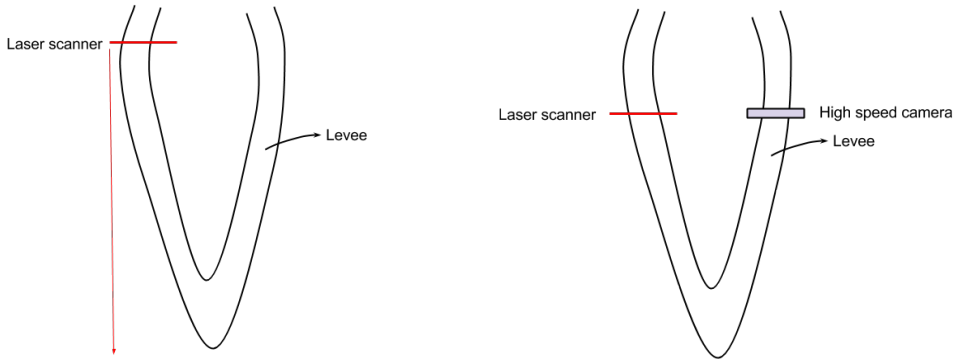

(a) Laser scanner measurement (b) High speed camera position

Figure 8.7: Measurement setup

To visualise the measurements of the laser scanner, a high speed camera will be mounted on the other side of the flow (figure 8.7(b). It is assumed the levees on both sides of the flow are identical. It is tried to match the data from the laser scanner with the images from the high speed camera. The visualisation using the high speed camera should lead to a better qualitative understanding of the forming. In addition, it is possible to derive a velocity field from the high speed camera data. The velocity profile can be used to study differences between the given configurations. It might give an insight in the speed of segregation and the formation of levees.

The laser scanner can only give data about the contour of the levee. In order to study the internal structure of the levee five cross sections will be made visible. To visualise the structure a transparent piece of plastic is carefully placed in the deposit. With a fine brush, the ballotini on the lower side of the plastic is removed. A scale will be added on the plastic, in order to make a comparison between different cross sections. Pictures will be taken in order to make the comparison. In each deposit, five cross sections will be taken. Figure 8.8 shows the distribution of cross sections over the deposit. The position of the first cross section is chosen at the point where the side levees collide with the front levees. For this research the levee on the front is not of interest, so cross section 1 is the first point of interest. The last point of interest, is the point

where the influence of the first collapse is neglectable. Since it is hard to determine this point, it is chosen to take the point where the flow is widest. This is some distance away from the compartment, but still high upstream and easy to detect for all the different flows. In between, three cross sections are taken to study the development of the levees. Only three sections are taken, because changes are expected to be small and would be hard to notice with an increase of sections.

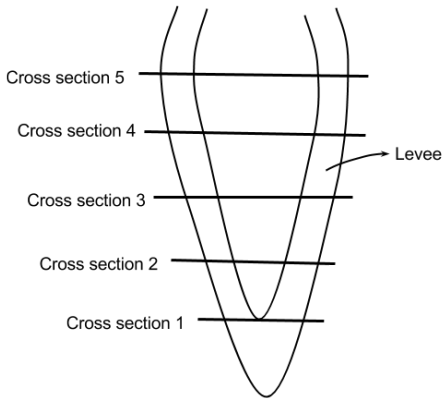

Figure 8.8: Cross sections

Until now, it was assumed the only influence was the size of particles. In order to check this assumption some additional experiments are executed. First of all, the particles will be poured into the compartment in a certain order. In the first run the big particles will be on the bottom, and the smaller particles on top. In the second run this order will be reversed. These experiments will show the influence of the initial state of the ballotini. The same measurements will be taken as in earlier proposed experiments.

Second, an uniform sample of ballotini will be used. It is believed levees will also form when particles are of the same size [5].In order to see the difference between levees formed by size segregation and levees formed by uniform sized particles this experiment is executed. Again, the same measurements will be taken.

Subsequent research

- Size segregation with 3 differently sized particles
- Levee forming on front
- Altering ratio big/small particles

Appendix D, Future research

1. Investigation into the basal friction for particles with d $> 2d_c$.
   Reasoning from the results of my experiments I would suggest there may exist another d_c, at which the basal friction is minimum. Changing only the roughness of the base can facilitate this study. However, the behaviour of the present 0.15 - 0.25 sample seems very different from all other size samples. The cause is unclear, so it is worth considering using the 0.3 - 0.4 mm red ballotini instead. In addition, the deposit thickness for all ballotini sizes on two different rough planes could be compared. In the study of Goujon et al [3] they only investigate this for one particle size (figure 11 in [3]). A broader approach may give a better overall understanding of the influence of the basal friction in relation to particle size.
2. Study of the influence of the ratio of small and large beads on the occurance of instabilities.
   My experiments were performed only using a 50-50% mixture of large and small beads. However, in a not recorded experiment with a 60% small bead mixture, a finger of small particles was breaking through the front formed of large particles. Subsequently, the influence of the mixing procedure can be taken into account.
3. Research into the increased mobility for several samples with differing ratios of basal friction and mixture.
   As mentioned before, I only performed experiments using a 50-50% mixture of large and small particles and altering this mixing ratio may lead to different results. Moreover, I only tested three different mixtures and expanding this with one or two mixtures could offer a better insight in the mechanism of increased mobility.
4. Investigation into the occurrence of roll waves at large inclination without the presence of a steady flow at smaller inclinations.
   In the 0.15 - 0.25 mm sample in this study roll waves were observed, but a steady flow at low inclinations was absent. The appearance of roll waves has been studied earlier [5,7,22], but the studied material always showed steady flow patterns at low inclinations.